

Solution for the BFKL Pomeron Calculus in zero transverse dimensions

M. Kozlov* and E. Levin†

*Department of Particle Physics, School of Physics and Astronomy
Raymond and Beverly Sackler Faculty of Exact Science
Tel Aviv University, Tel Aviv, 69978, Israel*

ABSTRACT: In this paper the exact analytical solution is found for the BFKL Pomeron calculus in zero transverse dimensions, in which all Pomeron loops have been included. The comparison with the approximate methods of the solution is given, and the kinematic regions are discussed where they describe the behaviour of the scattering amplitude quite well. In particular, the semi-classical approach is considered, which reproduces the main properties of the exact solution at large values of rapidity ($Y \geq 10$). It is shown that the mean field approximation leads to a good description of the scattering amplitude only if the amplitude at low energy is rather large. However, even in this case, it does not lead to the correct asymptotic behaviour of the scattering amplitude at high energies.

KEYWORDS: BFKL Pomeron, Generating functional, Semi-classical solution, Sturm-Liouville problem, Exact solution .

*Email: kozlov@post.tau.ac.il;

†Email: leving@post.tau.ac.il, levin@mail.desy.de;

Contents

1. Introduction	2
2. The equation and its general properties	3
2.1 The equation and initial and boundary conditions.	3
2.2 General properties of the Sturm-Liouville problem	5
2.3 The iterative algorithm for a search of the solution	7
3. Analytical solution to the Sturm-Liouville problem	10
3.1 Semi-classical approach	10
3.2 Exact solution at $u \rightarrow 1$	15
3.3 Approximate method	18
4. The exact solution to the problem	18
5. Numerical estimates	20
6. Comparison with approximate approaches	21
6.1 Exact solution and the semi-classical approach	21
6.2 Exact solution and the mean field approximation (MFA)	22
6.3 Exact solution and the Mueller-Patel-Salam -Iancu (MPSI) approximation.	24
6.4 Exact solution and the gray disc behaviour.	25
7. Conclusions	27
A. Appendix A: General way for solving linear nonhomogeneous boundary problem.	28
B. Appendix B: The exact semi-classical solution.	30
C. Appendix C: Hermitian Hamiltonian description of rapidity Hamiltonian.	31
D. Appendix D: The exact solution as a power series in rapidity	33

1. Introduction

It is well known that the BFKL Pomeron calculus [1, 2] gives the simplest and the most elegant approach to the high energy amplitude in QCD. This approach is based on the BFKL Pomeron [3] and the interactions between the BFKL Pomerons [4, 5, 6, 7], which are taken into account in the spirit of the Gribov Reggeon Calculus [8]. It can be written in the form of the functional integral (see Ref. [5]) and formulated in terms of the generating functional (see Refs. [9, 10, 11, 12, 13]). However, in spite of the fact that we have learned a lot about the properties of the high energy asymptotic behaviour at high energies, even the simplest case of the BFKL Pomeron in zero transverse dimension (a toy model, see Refs. [9, 12, 13]) has not been solved¹. In this paper we develop the analytical approach to this problem and find the solution. We hope that this solution will help us to develop a technique for the general approach in which the amplitude depends on the size of interacting dipoles as well as on their impact parameters.

The simple toy model has some advantages which makes it a good laboratory for seeking the solutions that include the Pomeron loops. First of all, the mean field approximation [1, 2, 16, 17] for this model has a simple analytical solution [10, 11] while it is a difficult problem in the general case and we have only few analytical approaches [18, 19], therefore, we have to rely very often (too often) on the numerical solutions [20]. The JIMWLK approach [30] coincides with the Balitsky-Kovchegov [17] one in this model making our life simpler in the mean field approach.

The first corrections due to the Pomeron loops which were suggested in Ref. [27, 28] can be easily summed in this model [29] giving a guide for the general impact of the Pomeron loops on the high energy asymptotic behaviour of the scattering amplitude.

We are aware that we can lose the important property of the QCD approach (see Refs. [31, 32, 33, 34, 35]) but we believe that the analytical solution to the simple model is a necessary step in finding more general and certainly more complicated solutions. We are certain that methods developed for solving this model, will be useful for searching for a general solution of this challenging and difficult problem.

The paper is organized as follows. In the next section we discuss the general properties of the equation that we need to solve. Being a diffusion equation this equation could be rewritten as the Sturm-Liouville equation which has a discrete spectrum. In section 3 we develop the semi-classical approach which results in finding the analytical solution to the equation. We show that this solution approaches the so called asymptotic solution at high energies. In this section we discuss the analytical solution at $u \rightarrow 1$ which gives the transparent example of the main properties of the general solution.

¹Some progress has been made in Refs. [13, 14, 15] and we will comment on these efforts below.

In section 4 we find the general analytical solution to the problem. We state that the prolate spheroidal wave functions is the complete set of the eigenfunctions of the master equation and build the Green function as well as solution to the master equation that satisfy the initial and boundary conditions that has been discussed in section 2.

In conclusions we discuss our results and check the approximate approaches, developed for this kind of equations, against the exact solution.

2. The equation and its general properties

2.1 The equation and initial and boundary conditions.

In the toy model the equation for the generating functional² has a simple form [9, 12, 13]

$$\frac{\partial Z}{\partial \mathcal{Y}} = u(1-u) \left(-\kappa \frac{\partial Z}{\partial u} + \frac{\partial^2 Z}{\partial u^2} \right) \quad (2.1)$$

where

$$\mathcal{Y} = \Gamma(2 \rightarrow 1) Y = (\Gamma(1 \rightarrow 2)/\kappa) Y \quad (2.2)$$

with vertex $\Gamma(2 \rightarrow 1)$ which describes a merging of two dipoles into one dipole. κ is the large parameter of our problem and it is equal to

$$\kappa = \frac{2 \cdot \Gamma(1 \rightarrow 2)}{\Gamma(2 \rightarrow 1)} = \frac{1}{\alpha_S^2} \gg 1 \quad (2.3)$$

where α_S is QCD coupling and $\Gamma(1 \rightarrow 2) = (N_c/\pi)\alpha_S = \bar{\alpha}_S$ is the vertex for the decay of the dipole into two dipoles. The order of these vertices $\Gamma(1 \rightarrow 2)$ and $\Gamma(2 \rightarrow 1)$ are chosen from the general equation for the generating functional in QCD (see Ref. [12] for example).

Eq. (2.1) is a typical diffusion equation with the diffusion coefficient that depends on variable u . We need to add an initial and boundary condition to solve such kind of equation. Generally, this equation describes the interaction between Pomerons with intercept $\Delta_P = \Gamma(1 \rightarrow 2) = \bar{\alpha}_S$. The Pomeron diagrams that describes Eq. (2.1) are shown in Fig. 1.

In this paper we are going to calculate the sum of enhanced diagrams (see Fig. 1) and for them we have the following initial condition³

$$Z(Y=0; u) = u \quad (2.4)$$

Since the physical meaning of Z is

$$Z(Y; u) = \sum_{n=0}^{\infty} P_n(Y) u^n \quad (2.5)$$

²Actually for the toy model, in which there is no dependence on the sizes of interacting dipoles, the generating functional degenerates to the generating function.

³In Eq. (2.4) as well everywhere below we use the notation Y for \mathcal{Y} . Hopefully it will not lead to troubles in understanding.

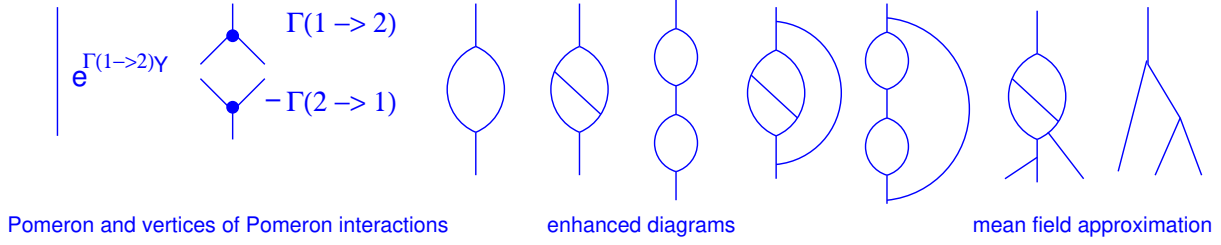


Figure 1: The Pomeron diagrams that are summed by Eq. (2.1). Solid lines denote the Pomerons. The first three diagrams show the Pomeron and vertices of Pomeron interaction. The next five diagrams are the examples of so called enhanced diagrams which we are going to sum in this paper. The last two diagrams give the example of the Pomeron diagrams in the mean field approximation.

where $P_n(Y)$ is the probability to find n -dipoles (or/and n -Pomerons) at rapidity Y . Therefore, Eq. (2.4) means that at low energies we have only one Pomeron.

The master equation (see Eq. (2.1)) describes Markov's chain for the probabilities $P_N(Y)$, namely [31, 12]

$$\begin{aligned} \frac{dP_n(Y)}{dY} = & -\Gamma(1 \rightarrow 2) n P_n(Y) + \Gamma(1 \rightarrow 2) (n-1) P_{n-1}(Y) \\ & - \Gamma(2 \rightarrow 1) \frac{n(n-1)}{2} P_n(Y) + \Gamma(2 \rightarrow 1) \frac{n(n+1)}{2} P_{n+1}(Y) \end{aligned} \quad (2.6)$$

Eq. (2.6) has a simple structure: for every process of dipole splitting or merging we see two terms. The first one with the negative sign describes a decrease of probability P_n due to the process of splitting or merging of dipoles. The second term with positive sign is responsible for the increase of the probability due to the same processes of dipole interactions.

The boundary conditions are very simple

$$Z(Y; u=1) = \sum_{n=0}^{\infty} P_n(Y) = 1 \quad (2.7)$$

which directly follows from Eq. (2.5) and express the conservation of probabilities, saying that the total probability is equal to unity at any value of rapidity.

Using the Laplace transform

$$Z(Y; u) = \int_{a-i\infty}^{a+i\infty} \frac{d\omega}{2\pi i} Z(\omega; u) e^{\omega Y} \quad (2.8)$$

we can reduce Eq. (2.1) to the following equation ⁴

$$\frac{\omega}{u(1-u)} Z(\omega; u) = -\kappa Z'_u(\omega; u) + Z''_{u,u}(\omega; u) \quad (2.9)$$

⁴In principle, this equation contains an inhomogeneous term (initial condition) $Z(Y=0, u)$, however, we will incorporate the correct initial condition later, after solving this homogeneous equation.

Introducing new functions

$$s(u) \equiv \frac{1}{u(1-u)} e^{-\kappa u}; \quad \text{and} \quad p(u) \equiv e^{-\kappa u}; \quad (2.10)$$

we can reduce Eq. (2.9) to the typical Sturm-Liouville equation [21, 22]

$$-s(u) \omega Z(\omega, u) + \frac{d}{du} (p(u) Z_u(\omega, u)) = 0 \quad (2.11)$$

2.2 General properties of the Sturm-Liouville problem

It is very instructive to remind ourselves of the general properties of the Sturm-Liouville problem which has been studied by mathematicians for a long time [21, 22].

1. Eq. (2.11) has the infinite set of the eigenvalues $\omega_n = -\lambda_n$. All λ_n are real and can be ordered so that $\lambda_1 < \lambda_2 < \lambda_3$ with $\lambda_n \rightarrow +\infty$. Therefore, there can exist only a finite number of negative λ_n . But for our particular case, (for Eq. (2.11)) there are no negative eigenvalues λ_n and $\lambda_1 = 0$ is the least eigenvalue, to which there corresponds the eigenfunction $Z_0(u) = \text{Constant}$;
2. The multiplicity of each eigenvalue is equal to 1;
3. The eigenvalues are determined up to a constant multiplier.
4. Each eigenfunction $Z_n(u)$ has exactly $n - 1$ zeroes in the interval $(0, 1)$;
5. Eigenfunctions $Z_n(u)$ and $Z_m(u)$ are orthogonal with weight $s(u)$, namely,

$$\int_0^1 du s(u) Z_n(u) Z_m(u) = 0 \quad \text{for} \quad n \neq m \quad (2.12)$$

6. An arbitrary function $F(u)$, that has a continuous derivative and satisfies the boundary conditions of the Sturm-Liouville problem (in other words, a function that we, as physicists, want to find), can be expanded into absolute and uniformly convergent series in eigenfunctions:

$$F(u) = \sum_{n=1}^{\infty} F_n Z_n(u); \quad \text{where} \quad F_n = \frac{1}{\|Z_n\|} \int_0^1 du' F(u') Z_n(u') \quad (2.13)$$

where

$$\|Z_n\|^2 = \int_0^1 du s(u) Z_n^2(u) \quad (2.14)$$

7. The following asymptotic relation holds for large eigenvalues as $n \rightarrow \infty$:

$$\lambda_n = \frac{\pi^2 n^2}{\Delta^2} + O(1); \quad \text{where} \quad \Delta = \int_0^1 \sqrt{\frac{s(u)}{p(u)}} du; \quad (2.15)$$

8. In our case (see Eq. (2.10))

$$\Delta = \int_0^1 \frac{du'}{\sqrt{u'(1-u')}} = \pi, \quad (2.16)$$

and, therefore, at large n

$$\lambda_n = n^2 \quad (2.17)$$

In Appendix E we compare this asymptotic spectrum with the spectrum of the exact solution as well as with the perturbation procedure to calculate it, given in the next section.

9. In our case we can use Eq. (2.17) and Eq. (2.15) for $n \gg 1$ to estimate not only the values of λ_n but also to find the corresponding eigenfunctions. These eigenfunctions have the following form:

$$\frac{Z_n(u)}{\|Z_n\|} = \left(\frac{4}{\pi^2} u(1-u) \right)^{\frac{1}{4}} e^{\frac{\kappa}{2} u} \sin(n \Theta(u)) + O\left(\frac{1}{n}\right) \quad (2.18)$$

where

$$\Theta(u) = - \int_u^1 \frac{du'}{\sqrt{u'(1-u')}} = -\frac{\pi}{2} - \arcsin(1-2u) \quad (2.19)$$

Introducing a more general equation ⁵ than Eq. (2.11), namely,

$$s(u) \frac{\partial Z(Y, u)}{\partial Y} = \frac{\partial}{\partial u} \left(p(u) \frac{\partial Z(Y, u)}{\partial u} \right) + \Phi(Y, u) \quad (2.20)$$

where $\Phi(Y, u)$ is a given function. We can find a general solution to this equation with the initial condition:

$$Z(Y=0, u) = f(u) \quad (2.21)$$

and with the boundary conditions:

$$Z(Y, u=0) = 0; \quad (2.22)$$

$$Z(Y, u=1) = 1; \quad (2.23)$$

The form of this solution is (see section **1.8.9** in Ref. [22])

$$\begin{aligned} Z(Y, u) &= \int_0^Y dY' \int_0^1 d\xi \Phi(Y', \xi) G(Y - Y'; u, \xi) + \int_0^1 d\xi s(\xi) f(\xi) G(Y; u, \xi) \\ &+ p(u=1) \int_0^Y dY' Z(Y, u=1) \frac{\partial G(Y - Y'; u, \xi)}{\partial \xi} \Big|_{\xi=1} \\ &+ p(u=0) \int_0^Y dY' Z(Y, u=0) \frac{\partial G(Y - Y'; u, \xi)}{\partial \xi} \Big|_{\xi=0} \end{aligned} \quad (2.24)$$

⁵More useful information on the general Sturm-Liouville is given in Appendix A and in Refs.[21, 22, 23].

where the Green function of this equation is equal to

$$G(Y; u, \xi) = \sum_{n=1}^{\infty} \frac{Z_n(u) Z_n(\xi)}{\|Z_n\|^2} e^{-\lambda_n Y} \quad (2.25)$$

where Z_n are the eigenfunction of Eq. (2.11) with the boundary conditions

$$Z_n(u=0) = 0; \quad Z_n(u=1) = 0; \quad (2.26)$$

One can see that we know a lot about the properties of the master equation.

2.3 The iterative algorithm for a search of the solution

The general formula, given in the previous section, leads to a definite algorithm for numerical calculations. In the first stage of this algorithm we can use the eigenvalues given by Eq. (2.17), and the eigenfunctions from Eq. (2.18). The Green function has the form

$$G_{\infty}(Y; u, \xi) = \frac{2}{\pi} \sqrt{\sin \Theta(u) \sin \Theta(\xi)} e^{\frac{\kappa}{2}(u+\xi)} \sum_{n=-\infty}^{n=\infty} \exp(i n \{ \Theta(u) - \Theta(\xi) \}) e^{-n^2 Y} \quad (2.27)$$

The solution can be found from Eq. (2.24) and it has the form

$$\begin{aligned} Z_{\infty}(Y, u(\Theta)) &= \int_0^Y dY' \int_{-\pi}^0 d\Theta' \frac{\frac{1}{2}(\cos \Theta' + 1)}{\sin \Theta'} e^{-\kappa u(\Theta)} G_{\infty}(Y - Y'; u(\Theta), \xi(\Theta')) - \\ &- e^{-\kappa} \int_0^Y dY' \frac{\partial G_{\infty}(Y - Y'; u(\Theta), \xi(\Theta'))}{\partial \xi(\Theta')} \Big|_{\Theta'=0} \end{aligned} \quad (2.28)$$

In the next stage of the algorithm we are searching for the solution in the form

$$Z(Y, u) = \Delta Z(Y, u) + Z_{\infty}(Y, u) \quad (2.29)$$

and for $\Delta Z(\omega, u)$ we obtain the following equation

$$-s(u)\omega \Delta Z(\omega, u) = L(\Delta Z(\omega, u)) + L(Z_{\infty}(\omega, u)) \quad (2.30)$$

where we denote by L the Sturm-Liouville operator, namely $L = \frac{d}{du} \left(p(u) \frac{d}{du} \right)$.

Eq. (2.30) is prepared for the iterative procedure of finding the solution using Eq. (2.28) as the first iteration. To calculate the second iteration we substitute $Z_{\infty}(Y, u)$ into Eq. (2.30) which has the form of Eq. (2.20) with $\Phi(Y, u) = L(Z_{\infty}(Y, u))$. Using Eq. (2.24) we can find $\Delta Z(Y, u)$. Repeating this procedure several times we will obtain the numerical solution to the problem. However, the procedure would be better converged if we could determine the eigenvalues of the problem at small values of n . Below we suggest two approximations that allows us to approach small values of n .

The algorithm described above has a very simple meaning if we re-write our equation as a Schroedinger-type equation. It is easy to see that the search for $Z_\infty(Y, u)$ of Eq. (2.28) can be simplified if we introduce a new function T

$$Z(Y, u) = T(Y, \Theta) e^{\frac{\kappa}{2} u} \quad (2.31)$$

For this function we can rewrite Eq. (2.9) in the very convenient form for the function $T(Y, \Theta)$ introducing a new variable Θ (see Eq. (2.19)) instead of u .

$$\frac{\omega}{\sin \Theta} T(\omega, \Theta) = -\frac{\kappa^2}{4} \sin \Theta T(\omega, \Theta) + \frac{d}{d\Theta} \frac{1}{\sin \Theta} \frac{dT(\omega, \Theta)}{d\Theta} \quad (2.32)$$

which is a generalized Sturm - Liouville equation of the form

$$s(\Theta) \frac{\partial T(Y, \Theta)}{\partial Y} = \frac{\partial}{\partial \Theta} p(\Theta) \frac{\partial T(Y, \Theta)}{\partial \Theta} - q(\Theta) T(Y, \Theta) \quad (2.33)$$

with

$$s(\Theta) = 1/\sin \Theta; \quad p(\Theta) = 1/\sin \Theta; \quad q(\Theta) = \frac{\kappa^2}{4} \sin \Theta \quad (2.34)$$

Eq. (2.33) allows us to find corrections of the order of $1/n^2$ to the spectrum of the Sturm - Liouville operator. Indeed, λ_n is equal to (see section **1.8.9** in Ref. [22])

$$\sqrt{\lambda_n} = n + \frac{1}{\pi n} Q(0, -\pi) + O\left(\frac{1}{n^2}\right) \quad (2.35)$$

where

$$Q(\Theta, \Theta') = \frac{1}{2} \int_{\Theta'}^{\Theta} d\Theta'' q(\Theta'') = \frac{\kappa^2}{8} \{\cos \Theta' - \cos \Theta\} \quad (2.36)$$

The estimate for the eigenfunctions looks as follows

$$T_n(\Theta) = \sin(n\Theta) - \frac{\kappa^2}{4\pi n} \{2\Theta + \pi(1 - \cos \Theta)\} \cos(n\Theta) + O\left(\frac{1}{n^2}\right) \quad (2.37)$$

Eq. (2.32) can be re-written as a Schroedinger-type equation:

$$\frac{d^2 \Psi}{(d\Theta)^2} + (E - U(\Theta)) \Psi = 0. \quad (2.38)$$

Indeed, Eq. (2.32) has the equivalent form

$$\omega T = -\frac{\kappa^2}{4} \sin^2 \Theta T - \cot \Theta T_\Theta + T_{\Theta\Theta} \quad (2.39)$$

Introducing (see Appendix C for general way of reducing the Fokker-Planck equation to the evolution described by hermitian Hamiltonian)

$$T = \phi(\Theta) \Psi(\Theta) \quad \text{with} \quad \phi(\Theta) = \sqrt{\sin \Theta} \quad (2.40)$$

we obtain for Ψ the Schroedinger equation with

$$E = -\omega ; \quad \text{and} \quad (2.41)$$

$$U(\Theta) = \frac{\kappa^2}{4} \sin^2 \Theta + \frac{1}{4} (2 + 3 \cot^2 \Theta) ;$$

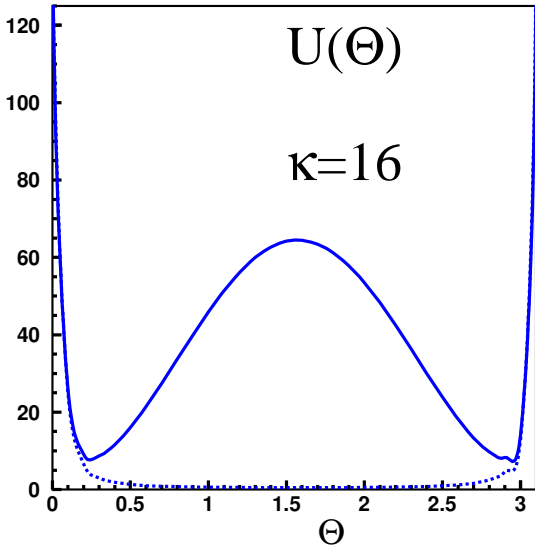


Figure 2: The potential energy $U(\Theta)$ of Eq. (2.41) versus Θ at $\kappa=16$, . The dashed line shows the potential $U(\Theta) - (\kappa^2/4) \sin^2 \Theta$ which corresponds to the set of the eigenfunctions given by Eq. (2.18).

In Fig. 2 we plot this potential. One can see that for large κ it has a typical two minima form with the maximum at $\Theta = \pi/2$ while at $\Theta \rightarrow 0$ and $\Theta \rightarrow \pi$ $U(\Theta)$ increases approaching infinity.

Therefore, for large energy excitation we can replace this potential by the rectangular-well potential with the wave functions given by Eq. (2.18) with the spectrum of Eq. (2.15). Indeed, Fig. 2 shows that $U(\Theta) - \frac{\kappa^2}{4} \sin^2(\Theta) = \frac{1}{4} (2 + 3 \cot^2 \Theta)$ denoted as dashed line, can be replaced by the potential which is equal to zero for $0 < \Theta < 2\pi$ and which is infinitely large outside of this region. Such potential allows us to reduce Eq. (2.38) to the Schroedinger equation with the simplified potential, namely,

$$\frac{d^2 \Psi}{(d\Theta)^2} + \left(E - \frac{\kappa^2}{4} \sin^2(\Theta) \right) \Psi = 0 ; \quad \text{with} \quad \Psi(\Theta=0) = \Psi(\Theta=2\pi) = 0 \quad (2.42)$$

The boundary conditions in Eq. (2.42) reflects the fact that potential is very large outside the $[0, 2\pi]$ interval in Θ .

The fact that we have two minima potential leads to the asymptotic behaviour of the amplitude which is determined by the asymptotic solution of Eq. (2.9) for $\omega = 0$ (see Refs.[13, 40, 41]), namely,

$$Z_{asympt}(Y = \infty, u) = \frac{1 - e^{\kappa u}}{1 - e^{\kappa}} \quad (2.43)$$

which satisfy both boundary conditions: $Z_{asympt}(u=0) = 0$ and $Z_{asympt}(u=1) = 1$.

In section 4 we will give the exact analytical solution to the master equation and we postpone until this section our discussion of this Schroedinger-type of the equation. However, this equation (see Eq. (2.38)) allows us to use the usual perturbative approach for the numerical solutions. For example we can represent the potential $U(\Theta)$ of Eq. (2.41) in the form

$$U(\Theta) = U_0(\Theta) + V(\Theta) \quad (2.44)$$

and solve Eq. (2.38) with U_0 exactly. Considering $V(\Theta)$ as being small we can develop the usual perturbation approach in quantum mechanics for a numerical solution of the equation. The value of κ is large in our

approach and we need to take such a perturbation procedure with a great precaution. In appendix E we give the spectrum of λ_n calculated in the first order of this doubtful perturbation procedure. The agreement with the exact spectrum is very impressive.

However for large values of κ the more reasonable way to find a good first approximation for searching Z_∞ is to use the semi-classical approach which we consider below.

3. Analytical solution to the Sturm-Liouville problem

3.1 Semi-classical approach

In our master equation (see Eq. (2.9)) we have a natural large parameter: κ (see Eq. (2.3)). We wish to use this parameter to develop a semi-classical approach to the master equation. We assume that

$$Z(\omega; u) = e^{\phi(\omega; u)} \quad \text{where} \quad \phi''_{u,u} \ll (\phi'_u)^2 \quad (3.1)$$

Substituting Eq. (3.1) into Eq. (2.9) one can reduce this equation to the form

$$\frac{\omega}{u(1-u)} = -\kappa \phi'_u + (\phi'_u)^2 \quad (3.2)$$

Solving Eq. (3.2) we obtain

$$\frac{d\phi_u^\pm}{du} = \frac{\kappa}{2} \left(1 \pm \sqrt{1 + \frac{4\omega}{\kappa^2 u(1-u)}} \right) \quad (3.3)$$

and

$$\phi^\pm(\omega; u) = - \int_u^1 \phi_{u'}^{\pm'}(\omega; u') du' \quad (3.4)$$

The general solution to Eq. (3.1) has the form

$$Z(Y; u) = \int_{a-i\infty}^{a+i\infty} \frac{d\omega}{2\pi i} e^{\omega Y} \left\{ \Phi^{(-)}(\omega) e^{\phi^-(\omega, u)} + \Phi^{(+)}(\omega) e^{\phi^+(\omega, u)} \right\} \quad (3.5)$$

where functions $\Phi^{(-)}(\omega)$ and $\Phi^{(+)}(\omega)$ should be found from initial and boundary conditions (see Eq. (2.4) and Eq. (2.7)). We recall that we use Y for $\mathcal{Y} = \Gamma(2 \rightarrow 1) Y$.

The contour of integration (contour C in Fig. 3) over ω is situated to the right of the singularities as it is shown in Fig. 3. As we have discussed the general structure of the singularities looks as follows. We have no singularities for positive $\omega = \omega_n^+ > 0$. It looks strange since one can see from Eq. (3.3) that we have a restricted number of singularities for positive $\omega = \omega_n^+ > 0$. However, since the contour of integration C in Fig. 3 is placed between $\omega_0 = 0$ and $\omega = \omega_1^+$, we can close it to the left semi-plane (left contour C_1 in Fig. 3). Therefore, the singularities ω_n^+ does not contribute to the integral of Eq. (3.5).

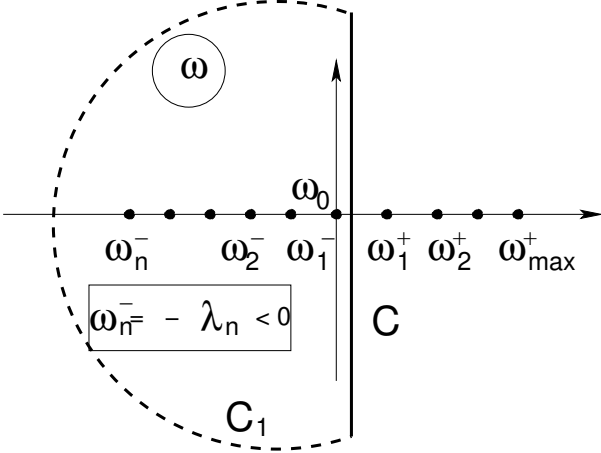


Figure 3: The contours of integration over ω in Eq. (3.5). All singularities are located along real negative real axis ($\omega_n = -\lambda_n < 0$)

Ref. [10], for example) one can see that all positive singularities ω^+ in Fig. 3) are the singularities of $\Phi^{(-)}$ while $\Phi^{(+)}$ has the singularities at the negative values of ω . Therefore, the only singularities that we need to take into account are those that are described by Eq. (3.6).

For $\omega \approx \kappa^2$ we need to expand the exact formulae for $\phi^\pm(\omega, u)$ in the kinematic region. For $\frac{\omega}{\kappa^2 u(1-u)} \gg 1$. In this region $\phi^\pm(\omega, u)$ are equal to

$$\phi^\pm(\omega, u) = \quad (3.8)$$

$$\frac{\kappa}{2}(u-1) \pm i\sqrt{|\omega|} \Theta(u) = \frac{\kappa}{2}(u-1) \pm i\mu_n \Theta(u)$$

where Θ is given by Eq. (2.19) and $\omega_n = -\lambda_n = -\mu_n^2$.

Therefore, in both branches ϕ^\pm we have singularities at negative ω and from estimates of Eq. (2.17) we know that $\lambda_n = n$. Using simple relations between variables u and Θ

$$u = \frac{1}{2} (\cos \Theta + 1); \quad (3.9)$$

we can rewrite $\exp(\phi^\pm(\omega, u))$ in the form

$$\exp(\phi^\pm(\omega_n = -\lambda_n = -\mu_n^2, u)) = \exp\left(\frac{\kappa}{8} \left[-2 + \zeta + \frac{1}{\zeta}\right]\right) \zeta^{\pm \mu_n} \quad (3.10)$$

where we introduce new variable

$$\zeta = e^{i\Theta} \quad (3.11)$$

It is obvious from Eq. (3.8) that ζ^n is the eigenfunction of our master equation at large values of ω ($\omega \geq \kappa$). However, the eigenfunctions that satisfy the boundary conditions of Eq. (2.26) are

$$Z_n(\Theta) = \sin(n\Theta) \quad (3.12)$$

The analytical function for Eq. (3.4) is written in the Appendix B while here we will discuss this function in two different limits: $\frac{\omega}{\kappa^2 u(1-u)} \ll 1$ and $\frac{\omega}{\kappa^2 u(1-u)} \gg 1$.

For $\frac{\omega}{\kappa^2 u(1-u)} \ll 1$ we have for function $\phi^\pm(\omega; u)$ the following expression

$$\phi^+(\omega; u) = \kappa(u-1) + \frac{\omega}{\kappa} \ln\left(\frac{u}{1-u}\right) \quad (3.6)$$

$$\phi^-(\omega; u) = -\frac{\omega}{\kappa} \ln\left(\frac{u}{1-u}\right); \quad (3.7)$$

It is easy to see that $\phi^+(\omega; u)$ of Eq. (3.6) corresponds to the solution which survives at $\kappa \rightarrow \infty$ which describes the case of the mean field approach. Analyzing the mean field solution (see

These functions form the complete set of functions in the interval $0 \leq u \leq 1$. In other words, the approximation of Eq. (2.17) turns out to be exact in our semi-classical approach. Having this fact in mind, we can find function $\Phi^{(\pm)}(\omega)$ in Eq. (3.5) from the initial condition of Eq. (2.4).

Functions ζ^n are eigenfunctions of Eq. (2.32) in which we neglect the first term in the r.h.s. and the second one is modified assuming that

$$\frac{d}{d\Theta} \frac{1}{\sin \Theta} \frac{d T(\omega, \Theta)}{d\Theta} \quad \text{is replaced by} \quad \frac{1}{\sin \Theta} \frac{d^2 T(\omega, \Theta)}{d\Theta^2}.$$

In this approximation Eq. (2.32) reduces to

$$\omega T(\omega, \Theta) = \frac{d^2 T(\omega, \Theta)}{d\Theta^2} \quad (3.13)$$

It is easy to see that Eq. (3.12) gives the eigenfunctions of this equation.

Using the solution of Eq. (3.13) we can calculate the Green function for our master equation (see Eq. (2.9)) that this Green function has a very simple form, namely

$$G_{\infty}^{SC}(Y; \Theta, \Theta') = \frac{1}{\pi} e^{\frac{\kappa}{2} + \frac{\kappa}{4} [\cos \Theta + \cos \Theta']} \sum_{n=1}^{\infty} \sin(n\Theta) \sin(n\Theta') e^{-n^2 Y} \quad (3.14)$$

and the initial conditions have the form

$$T(Y=0, \Theta) = \frac{1}{2} (1 + \cos \Theta) \exp\left(-\frac{\kappa}{4} (1 + \cos \Theta)\right) \quad (3.15)$$

Using this Green function we obtain the semi-classical solution in the form

$$Z_{\infty}^{SC} = \frac{1}{\pi} \sum_{n=-\infty}^{\infty} \left\{ e^{-n^2 Y} e^{\frac{\kappa}{2} u} \sin(n\Theta) \int_{-\pi}^0 d\Theta' \sin(n\Theta') \frac{1}{2} (1 + \cos \Theta') \exp\left(-\frac{\kappa}{4} (1 + \cos \Theta')\right) \right\} \quad (3.16)$$

The integral over Θ' could be taken using the generating function for the modified Bessel function of the first kind (see formula **9.6.33** in Ref.[25])

$$\exp\left(\frac{\kappa}{4} \cos \Theta\right) = \sum_{n=-\infty}^{\infty} I_n\left(\frac{\kappa}{4}\right) e^{in\Theta} \quad (3.17)$$

and the expression for simple integral

$$\int_{-\pi}^0 d\Theta' \cos(n\Theta') \sin(k\Theta') = -\frac{k(1 - (-1)^{n+k})}{k^2 - n^2} \quad (3.18)$$

From Eq. (3.17) and Eq. (3.18) one can derive that

$$C(n, \kappa) = \int_{-\pi}^0 d\Theta' \sin(n\Theta') \frac{1}{2} (1 + \cos \Theta') \exp\left(-\frac{\kappa}{4} (1 + \cos \Theta')\right) = \frac{1}{2} \exp(-\kappa/4) \times \quad (3.19)$$

$$\left\{ \sum_{m=1}^{\infty} (I_{m+1}(-\kappa/4) + I_{m-1}(-\kappa/4) + 2I_m(-\kappa/4)) \frac{n(1 - (-1)^{n+m})}{n^2 - m^2} + (I_1(-\kappa/4) + 2I_0(-\kappa/4)) \frac{(-1)^n - 1}{n} \right\}$$

Substituting Eq. (3.19) into Eq. (3.16) we obtain

$$Z_{\infty}^{SC} = \frac{1}{\pi} e^{\frac{\kappa}{2}(u-1)} \left(C(0, \kappa) + 2 \sum_{n=1}^{\infty} \left\{ e^{-n^2 Y} e^{\frac{\kappa}{2} u} \sin(n \Theta) C(n, \kappa) \right\} \right) \quad (3.20)$$

However, this expression for Z_{∞}^{SC} has two disadvantages: (i) we approximate $\omega_n = -n^2$ even at small values of n where we know that our spectrum is different (see Eq. (3.6) and Eq. (3.7)); and (ii) $Z_{\infty}^{SC}(Y, u = 1) \neq 1$ (actually $Z_{\infty}^{SC}(Y, u = 1) = 0$).

The set of eigenfunction at small values of n is clear from Eq. (3.6) and Eq. (3.7), namely,

$$Z_n(u) = \begin{cases} \text{for } u \geq \frac{1}{2} & e^{\kappa(u-1)} \tau^n = \exp\left(\kappa \frac{\tau}{1-\tau}\right) \tau^n \text{ where } \tau = \frac{u-1}{u} \\ \text{for } u \leq \frac{1}{2} & \tau^n \text{ where } \tau = \frac{u}{u-1} \end{cases} \quad (3.21)$$

The fact that we have two different sets of the eigenfunctions for $u \geq 1/2$ and $u \leq 1/2$, directly comes from the contour integral of Eq. (3.5) and the expressions of Eq. (3.6) and Eq. (3.7) for functions ϕ^+ and ϕ^- . Indeed, for $u \geq 1/2$ $\ln(u/(1-u))$ is positive and we can close the contour in Eq. (3.5) to the left semi-plane for ϕ^+ . For $u \leq 1/2$ this log is negative and we have to use ϕ^- for negative values of ω . Recall, that we know from the general properties of the Sturm-Liouville equation that only negative ω contribute.

The value of $\omega_n = -\lambda_n$ for the eigenfunctions of Eq. (3.21) is equal to

$$\lambda_n = \kappa n \quad (3.22)$$

Coefficients $C(n, \kappa)$ we can find using the following series

$$u \exp(-\kappa(u-1)) = \frac{1}{1-\tau} \exp\left(-\kappa \frac{\tau}{\tau-1}\right) = \sum_{n=0}^{\infty} L_n(-\kappa) \tau^n \quad (3.23)$$

where $L_n(-\kappa)$ is the Laguerre polynomial (see formula **8.975** in Ref.[24]).

From Eq. (3.23) one can see that the initial condition $Z(Y = 0, u) = u$ can be re-written in the form of

$$u = \sum_{n=0}^{\infty} C(n, \kappa) Z_n(u) \Theta\left(u \geq \frac{1}{2}\right) \quad (3.24)$$

with $C(n, \kappa) = L_n(-\kappa)$.

We suggest to build the Green function considering for all $\lambda_n \leq \kappa^2$ the set of the eigenfunction given by Eq. (3.21) while for $\lambda_n > \kappa^2$ we use the set of Eq. (3.12).

It means that our Green function has the form

$$\begin{aligned}
G^{SC}(Y; u, \xi) = & \exp(\kappa(u + \xi - 2)) \sum_{n=0}^{n=[\kappa]+1} \tau(u) \tau(\xi) e^{-n\kappa Y} \\
& + \exp\left(\frac{\kappa}{2}(u + \xi - 2)\right) \sum_{n=[\kappa]+2}^{\infty} \sin(n\Theta(u)) \sin(n\Theta(\xi)) e^{-n^2 Y}
\end{aligned} \tag{3.25}$$

which leads to the generating function in the form

$$\begin{aligned}
Z^{SC}(Y; u) = & \Theta\left(u \geq \frac{1}{2}\right) \exp(\kappa(u - 1)) \sum_{n=0}^{n=[\kappa]+1} \tau(u)^n L_n(-\kappa) e^{-n\kappa Y} \\
& + \Theta\left(u \leq \frac{1}{2}\right) \sum_{n=0}^{n=[\kappa]+1} \tau(u)^n e^{-n\kappa Y} + \exp\left(\frac{\kappa}{2}(u - 1)\right) \sum_{n=[\kappa]+2}^{\infty} \sin(n\Theta(u)) C(n, \kappa) e^{-n^2 Y}
\end{aligned} \tag{3.26}$$

This solution has two problems which cannot be solved analytically: a dependence of the separation parameter between large and small n which was taken in Eq. (3.26) to be equal to $[\kappa] + 1$ and rather complicated expression for $C(n, \kappa)$ (see Eq. (3.19)) which does not allow us to make all calculation analytically. We investigated both problems computing Eq. (3.26) numerically for different separation parameters. It turns out that the answer is very insensitive to the exact value of the separation parameter if only we take it around κ . Actually, the value of this parameter we can find comparing exact semi-classical functions ϕ^\pm with our approximate ones (see Appendix B, where we discuss the exact functions).

The behaviour of the scattering amplitude is illustrated in Fig. 4 as a function of rapidity Y . In Fig. 5 one can see the u dependence of our solution at large values of rapidity Y . This behaviour confirms the expectation that has been discussed in Ref. [13], that at high energy our master equation predicts the gray disc behaviour for the scattering amplitude.

We check the accuracy of the semi-classical solution by calculating the following function:

$$\Delta(Y, u) = \frac{\left(\frac{\partial}{\partial Y} + \kappa u(1 - u) \frac{\partial}{\partial u} - u(1 - u) \frac{\partial^2}{(\partial u)^2} \right) Z^{SC}(Y, u)}{\text{minimal separate term of the numerator}} \tag{3.27}$$

As we have expected the semi-classical approach is rather bad at small values of $Y \leq 0.05$ leading to $\Delta(Y, u) \approx 40\%$ for $u \approx 0.5$. However, for large values of Y ($Y > 0.1$) the accuracy is better than 10 % for all values of u . It should be stressed that for $u > 0.8$ in the entire kinematic region of Y the accuracy is not worse than 10%. All estimates were done for $\kappa = 16$. This fact is very encouraging since the scattering amplitude N can be calculated in the following way [17, 11]

$$N(Y, \gamma(Y_0)) = 1 - Z(Y, u = 1 - \gamma(Y_0)) \tag{3.28}$$

where $\gamma(Y_0)$ is the scattering amplitude at low energy ($Y=0$). As it is discussed in Refs. [17, 11] in Eq. (3.28) we assume that n dipoles interact with the target independently. It means that the scattering amplitude of n dipoles with the target $\gamma_n(Y_0) = \gamma^n(Y_0)$. In our QCD motivated model $\gamma \approx 1/\kappa \ll 1$. Therefore, we are interested only in the values of u that are close to unity ($u \rightarrow 1$), where the semi-classical approach works quite well.

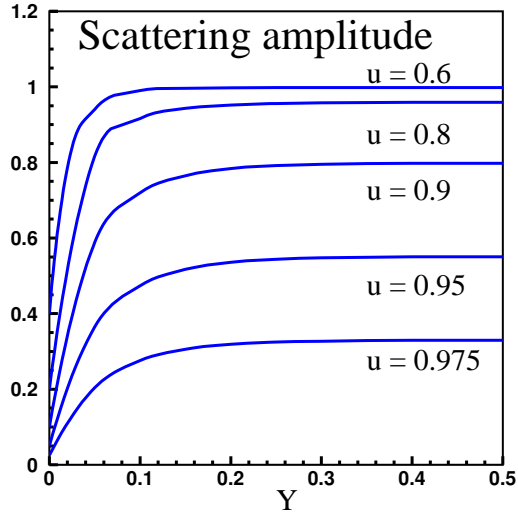


Figure 4: The dependence of the scattering amplitude versus rapidity at fixed $\kappa = 16$. Recall that here we denote $Y \equiv \mathcal{Y}$ (see Eq. (2.2)).

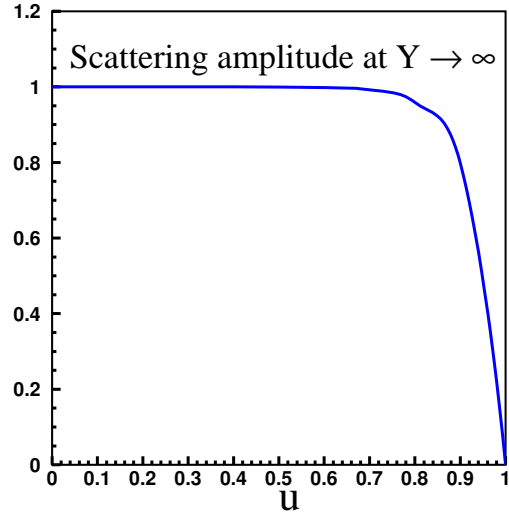


Figure 5: The asymptotic dependence of the scattering amplitude (see Eq. (3.26)) versus u at fixed $\kappa = 16$.

However, in the next section we develop a better analytical approach for such u .

3.2 Exact solution at $u \rightarrow 1$

To check that the eigenvalues in the region of small ω is determined by Eq. (3.22) we develop a different analytical approach. In the vicinity of $u = 1$ we can replace Eq. (2.1) by the following equation:

$$\frac{\partial Z}{\partial \mathcal{Y}} = (1-u) \left(-\kappa \frac{\partial Z}{\partial u} + u \frac{\partial^2 Z}{(\partial u)^2} \right) \quad (3.29)$$

For $Z(\omega, u)$ Eq. (3.29) reduces to the form

$$\omega Z(\omega, u) = -\kappa(1-u) Z_u(\omega, u) + u(1-u) Z_{uu}(\omega, u) \quad (3.30)$$

The solution to Eq. (3.30) is the Gauss's hypergeometric function

$$Z(\omega, u) = u^{1+\kappa} {}_2F_1(\alpha, \beta, \gamma, u) \quad (3.31)$$

(see formula **9.151** in Ref. [24]) with the following parameters

$$\begin{aligned}\alpha &= \frac{1}{2}(1 + \kappa) + \frac{1}{2}\sqrt{(1 + \kappa)^2 - 4\omega}; \\ \beta &= \frac{1}{2}(1 + \kappa) - \frac{1}{2}\sqrt{(1 + \kappa)^2 - 4\omega}; \\ \gamma &= \kappa + 2;\end{aligned}\tag{3.32}$$

The generating function that satisfies the boundary condition $Z(Y, u = 1) = 1$ is equal to

$$Z(\omega, u) = u^{1+\kappa} \frac{1}{\omega} \frac{{}_2F_1(\alpha, \beta, \gamma, u)}{{}_2F_1(\alpha, \beta, \gamma, u = 1)}\tag{3.33}$$

Since (see formula **9.122** in Ref. [24])

$${}_2F_1(\alpha, \beta, \gamma, u = 1) = \frac{\Gamma(\gamma) \Gamma(1)}{\Gamma(\gamma - \alpha) \Gamma(\gamma - \beta)}\tag{3.34}$$

The eigenvalues stem from the poles of $\Gamma(\gamma - \alpha)$ or $\Gamma(\gamma - \beta)$, namely, from the equation

$$\gamma - \alpha = -n; \quad \text{which gives} \quad \omega_n = -\lambda_n = -n^2 - n(1 + \kappa) \quad \text{where } n = 1, 2, 3, \dots\tag{3.35}$$

This equation leads to a smooth transition between large and small values of n supporting our semi-classical formula. Substituting Eq. (3.33) in Eq. (3.5) one can find the eigenfunction of our equation. They have the following form

$$Z_n(u) = \frac{1}{\|Z_n\|^2} u^{1+\kappa} P_n^{-1, 1+\kappa}(2u - 1)\tag{3.36}$$

where $P_n^{-1, 1+\kappa}$ are the Jacobi polynomials (see sections **8.960 - 8.967** in Ref. [24]).

The normalization of function Z_n in Eq. (3.36) is obvious since

$$\begin{aligned}\|Z_n\|^2 &= \\ \int_0^1 du \frac{u^{1+\kappa}}{1-u} (P_n^{-1, 1+\kappa}(2u - 1))^2 &= \frac{\Gamma(n) \Gamma(n + 2 + \kappa)}{n! (1 + \kappa + 2n) \Gamma(1 + \kappa + n)} = \frac{(n + 1 + \kappa)}{n(1 + \kappa + 2n)}\end{aligned}\tag{3.37}$$

It is easy to check that eigenfunctions of Eq. (3.36) satisfy the following boundary conditions;

$$Z_n(u = 0) = 0; \quad Z_n(u = 1) = 0\tag{3.38}$$

We found that the easiest way to solve the master equation (see Eq. (3.29)) is to introduce $Z(Y, u) = u + \tilde{Z}(Y, u)$. The equation for \tilde{Z} can be reduced to the Sturm-Liouville form, namely,

$$s(u) \frac{\partial \tilde{Z}}{\partial Y} = \frac{\partial}{\partial u} p(u) \frac{\partial \tilde{Z}}{\partial u} + \Phi(u)\tag{3.39}$$

where

$$s(u) = \frac{1}{u(1-u)} u^{-\kappa}; \quad p(u) = u^{-\kappa}; \quad \Phi(u) = -\kappa u^{-\kappa}\tag{3.40}$$

The solution to Eq. (3.39) has the form

$$\tilde{Z}(Y, u) = \int_0^Y dY' \int_0^1 d\xi G(Y - Y'; u, \xi) \Phi(\xi) \quad (3.41)$$

where

$$G(Y; u, \xi) = \sum_{n=1}^{\infty} \frac{Z_n(u) Z_n(\xi)}{\|Z_n\|^2} \exp(-\lambda_n Y) \quad (3.42)$$

where λ_n are given by Eq. (3.35) and Z_n is the set of the eigenfunction shown in Eq. (3.36).

In Fig. 6 we plotted the energy behaviour of the scattering amplitude for different values of u that are close to unity. One can see that this solution gives the amplitude which is quite different from the semi-classical solution. It sounds controversial, but actually it is not, since the solution of Eq. (3.41) contains the integral over ξ from 0 to 1 while our functions Z_n of Eq. (3.36) we know only at $u \rightarrow 1$.

It turns out that we can find a very simple solution at small values of u ($u \rightarrow 0$). Introducing a new variable $\gamma = 1 - u$ we can rewrite our master equation in the form at $\gamma \rightarrow 1$

$$\frac{\partial Z}{\partial \gamma} = (1 - \gamma) \left(\kappa \frac{\partial Z}{\partial \gamma} + \gamma \frac{\partial^2 Z}{(\partial \gamma)^2} \right) \quad (3.43)$$

or in ω -representation it looks as

$$\omega Z(\omega, \gamma) = (1 - \gamma) (\kappa Z_\gamma(\omega, \gamma) + \gamma Z_{\gamma\gamma}(\omega, \gamma)) \quad (3.44)$$

The solution to this equation has the form

$$Z(\omega, \gamma) = {}_2F_1(\alpha, \beta, \kappa, \gamma) = {}_2F_1(\alpha, \beta, \kappa, 1 - u) \quad (3.45)$$

where

$$\begin{aligned} \alpha &= \frac{1}{2} \left(\kappa - 1 + \sqrt{(1 - \kappa)^2 - 4\omega} \right); \\ \beta &= \frac{1}{2} \left((\kappa - 1) - \sqrt{(1 - \kappa)^2 - 4\omega} \right); \end{aligned} \quad (3.46)$$

The condition that gives us the spectrum of ω is

$$Z(\omega, 1 - u = 1) = {}_2F_1(\alpha, \beta, \kappa, 1) = \frac{\Gamma(\kappa) \Gamma(1)}{\Gamma(\kappa - \alpha) \Gamma(\kappa - \beta)} = 0 \quad (3.47)$$

The equation for the eigenvalues has the form

$$\kappa - \alpha = -n; \quad \text{which gives } \omega_n = -\lambda_n = n^2 + n(\kappa + 1) + 1 \quad \text{where } n = 0, 1, 2, \dots \quad (3.48)$$

One can see that this spectrum practically coincides with Eq. (3.35). Therefore, we can assume that Eq. (3.36) or Eq. (3.35) determines the spectrum of our problem in the entire region of u . This fact we will use below to develop the numerical approach to the master equation.

3.3 Approximate method

The semi-classical solution we can compare with a simpler approximation suggested in Ref. [13]. This approach consists of two steps. The first one is to find the asymptotic solution, namely, the solution to the following equation

$$-\kappa \phi'_u + (\phi'_u)^2 = 0 \quad (3.49)$$

This solution is $\phi_{asymp}(u) = \kappa(u-1)$ which satisfies the normalization $\phi(u=1) = 0$ that follows from $Z(u=1, Y) = 1$. The next step is to find a solution in the form $\phi(u; Y) = \phi_{asymp}(u) + \Delta\phi(u; Y)$ assuming that $\Delta\phi(u; Y) \ll \phi_{asymp}(u)$. The equation for $\Delta\phi(u; Y)$ is the typical Liouville equation

$$\frac{\partial \Delta\phi(u; Y)}{\partial Y} = \kappa u(1-u) \frac{\partial \Delta\phi(u; Y)}{\partial u} \quad (3.50)$$

with the initial condition

$$\Delta\phi(u; Y=0) = \ln(u) - \kappa(u-1) \quad (3.51)$$

The solution is an arbitrary function of the following type

$$\Delta\phi(u; Y=0) = H \left(Y + \frac{1}{\kappa} \ln \left(\frac{u}{1-u} \right) \right) \quad (3.52)$$

which can be found from the initial condition of

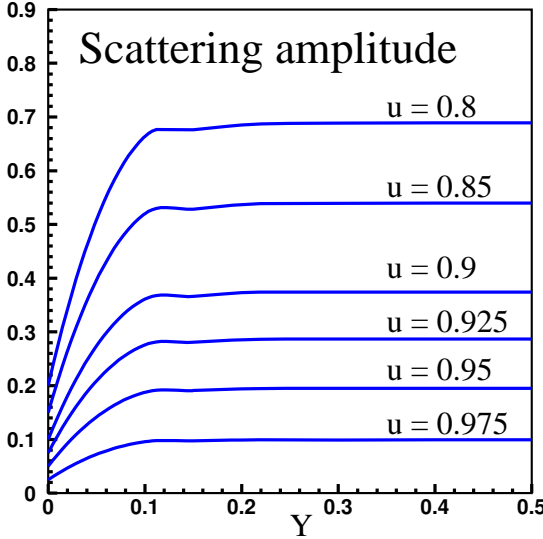


Figure 6: The scattering amplitude as a function of rapidity at different values of $u \rightarrow 1$. Recall that here we denote by $Y \equiv \mathcal{Y}$ (see Eq. (2.2)). κ is equal to 16 in this picture. Eq. (3.51).

The solution has the form

$$Z(u; Y) = \frac{u e^{\kappa Y}}{1 - u + u e^{\kappa Y}} \exp \left(\kappa u(1-u) \frac{1 - e^{\kappa Y}}{1 - u + u e^{\kappa Y}} \right) \quad (3.53)$$

This solution corresponds to the general solution, given by Eq. (3.26), but only one solution $\phi^+(\omega, u)$ is taken into account. In spite of the fact that the full semi-classical solution looks quite different from the simple expression of Eq. (3.53) the both solution are in less than 1% agreement at least for $\mathcal{Y} \geq 0.3$.

4. The exact solution to the problem

A master equation of Eq. (2.9) we can re-write in more convenient form, introducing a new function \mathcal{G} , namely ⁶,

$$Z(\omega, u) = e^{\frac{\kappa}{2}u} \mathcal{G}(v, \omega) u(1-u)$$

⁶One can see in Appendix C that Eq. (4.1) is a particular choice of the general transformation.

$$\begin{aligned}
&= \frac{1-v^2}{4} \mathcal{G}(v, \omega) e^{\frac{\kappa}{4}(1-v)} \\
\text{where } v &= 1 - 2u
\end{aligned} \tag{4.1}$$

For the function \mathcal{G} we have

$$\omega \mathcal{G}(\omega, v) = -\frac{\kappa^2}{16} (1-v^2) \mathcal{G}(\omega, v) + ((1-v^2) \mathcal{G}(\omega, v))_{vv} \tag{4.2}$$

The equation for \mathcal{G} can be re-written in the form

$$(1-v^2) \mathcal{G}_{vv} - 4v \mathcal{G}_v + \left\{ -\omega - 2 - \frac{\kappa^2}{16} (1-v^2) \right\} \mathcal{G} = 0 \tag{4.3}$$

For function $S_{n,m} = (1-v^2)^{\frac{m}{2}} \mathcal{G}(\omega, v)$ Eq. (4.3) reduces to the equation for the prolate spheroidal wave function with the fixed order parameter $m = 1$ and arbitrary degree parameter n which is an integer, $S_{n,m}(c, v)$ (see Refs. [25, 42]), namely,

$$\frac{d}{dv} \left((1-v^2) \frac{dS_{n,m}(c, v)}{dv} \right) + \left(\lambda_n^m - c^2 v^2 - \frac{m^2}{1-v^2} \right) S_{n,m}(c, v) = 0 \tag{4.4}$$

where

$$\begin{aligned}
\omega_n &= -\frac{\kappa^2}{16} - 2 + m(m+1) - \lambda_n^m = -\frac{\kappa^2}{16} - \lambda_n^m ; \\
m &= 1 ; \quad c^2 = -\frac{\kappa^2}{16} .
\end{aligned} \tag{4.5}$$

To verify Eq. (4.5) we can substitute $S_{n,m} = (1-v^2)^{\frac{m}{2}} \mathcal{G}(\omega, v)$ into Eq. (4.4) and obtain the following equation for function $\mathcal{G}(\omega, v)$

$$(1-v^2) \mathcal{G}_{vv} - 2(m+1)v \mathcal{G}_v + \{ \lambda_n^m - c^2 v^2 - m(m+1) \} \mathcal{G} = 0 \tag{4.6}$$

From Eq. (4.4) and Eq. (4.5) the set of the eigenfunctions for the generating function Z_n is equal to

$$Z_n = (1-v)^{\frac{1}{2}} S_{n,1}(i\frac{\kappa}{4}, v) e^{\frac{\kappa}{4}(1-v)} \tag{4.7}$$

The normalization of function $S_{n,1}$ is given by the following equations [25]

$$\|S_{n,1}(c, v)\|^2 = \int_{-1}^1 dv |S_{n,1}(c, v)|^2 = \frac{2n(n+1)}{2n+1} \tag{4.8}$$

The Green function of Eq. (4.4) has the form

$$G(Y - Y'; v, \xi) = \sum_{n=1}^{\infty} e^{-\lambda_n^1 (Y-Y')} \frac{S_{n,1}(i\frac{\kappa}{4}, v) S_{n,1}(i\frac{\kappa}{4}, \xi)}{\|S_{n,1}(i\frac{\kappa}{4}, v)\|^2} \tag{4.9}$$

It should be stressed that the Y dependence of the Green function is determined by the condition $E_n - E_{min} = -\omega_n + \omega_0 = \lambda_n^1$ in accordance with the Schroedinger equation (see Eq. (2.38)). $E_0 = -\omega_0$ is the lowest energy level which corresponds to the asymptotic state of Eq. (2.43). Therefore, Eq. (4.9) explicitly demonstrate that the generating function Z tends to $Z \rightarrow Z_{asympt}$ at high energies.

This Green function leads to the following formula for the generating function $Z(Y, u)$

$$Z(Y, u) = u + \quad (4.10)$$

$$\frac{u(1-u)}{\sqrt{1-(1-2u)^2}} e^{\frac{\kappa}{2} u} \sum_{n=1}^{\infty} \left(\frac{1 - e^{-\lambda_n^1 Y}}{\lambda_n^1} \right) \frac{S_{n,1}(i\frac{\kappa}{4}, 1-2u) \int_{-1}^1 d\xi S_{n,1}(i\frac{\kappa}{4}, \xi) \left(-\kappa \sqrt{1-\xi^2} e^{-\frac{\kappa}{4}(1-\xi)} \right)}{\|S_{n,1}(i\frac{\kappa}{4}, 1-2u)\|^2}$$

Fortunately, we have a rather detailed knowledge of the spheroidal functions in mathematics including the spectrum of λ_n^1 (see Refs. [25, 42]). The series in Eq. (4.10) is well converged and, practically, we need to take into account only about 10 terms.

Eq. (4.10) can be easily generalized for arbitrary initial condition: $Z(Y=0; u) = F(u)$.

Indeed, the solution has the form

$$Z(Y, u) = F(u) + \frac{u(1-u)}{\sqrt{1-(1-2u)^2}} \times \quad (4.11)$$

$$\times e^{\frac{\kappa}{2} u} \sum_{n=1}^{\infty} \left(\frac{1 - e^{-\lambda_n^1 Y}}{\lambda_n^1} \right) \frac{S_{n,1}(i\frac{\kappa}{4}, 1-2u) \int_{-1}^1 d\xi S_{n,1}(i\frac{\kappa}{4}, \xi) \left(\sqrt{1-\xi^2} L\left(F(\frac{1-\xi}{2})\right) e^{-\frac{\kappa}{4}(1-\xi)} \right)}{\|S_{n,1}(i\frac{\kappa}{4}, 1-2u)\|^2}$$

where L is the Sturm - Liouville operator defined in Eq. (2.30). In coming papers we will discuss the master equation with different initial conditions that reflect the interaction with nuclei and other targets [43, 44]

5. Numerical estimates

In our numerical calculations we use the package for mathematica written by P. Falloon (see Ref. [42]) which allows us to compute both the eigenvalues λ_n^1 and the spheroidal wave functions $S_{n,1}$ with fixed c given by Eq. (4.5). The result of our calculations at fixed $\kappa = 16$ which is related to the QCD coupling constant $\alpha_s = 0.25$, are plotted in Fig. 7 and Fig. 8.

Fig. 7 shows the generating function as function of u at different energies. One can see that at $\mathcal{Y} \gg 1$ the solution approaches the asymptotic solution of Eq. (2.43) (the low dashed line in Fig. 7) in accordance with our expectations [41, 40, 13]. To understand the scale of the energy dependence we need to go back to the rapidity Y from \mathcal{Y} . As we have discussed

$$Y = \frac{\kappa}{\Gamma(1 \rightarrow 2)} \mathcal{Y} = \frac{1}{\alpha_s^2 \omega_{BFKL}} \mathcal{Y} \quad (5.1)$$

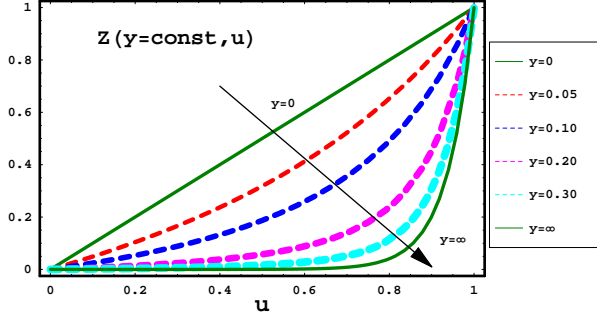


Fig. 7-a

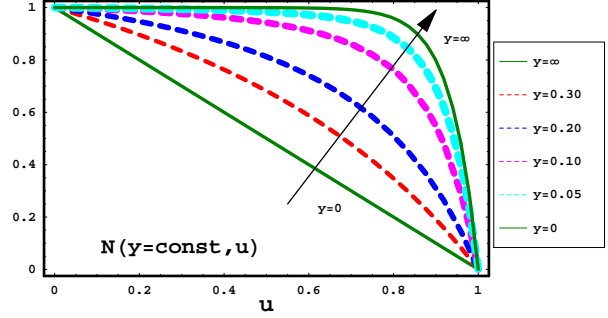


Fig. 7-b

Figure 7: The u dependence for the generating function $Z(Y, u)$ (Fig. 7-a) and the scattering amplitude $N(Y, u) = 1 - Z(Y, u)$ (Fig. 7-b) at different values of rapidity. In this figure we plot $Y \equiv \mathcal{Y}$ (see Eq. (2.2)). At $Y = \infty$ the asymptotic solution of Eq. (2.43) is shown. $\kappa = 16$.

where ω_{BFKL} is the intercept of the BFKL Pomeron[3], namely, $\omega_{BFKL} = 4 \ln 2 \bar{\alpha}_S$. For $\alpha_S = 0.25$ which we use in this paper, $Y = 23\mathcal{Y}$. Therefore, $\mathcal{Y} = 0.3$ gives $Y - Y_0 = 6.9$ (Y_0 is the initial rapidity from which we can apply our high energy approximation).

Fig. 8 shows the main result of this paper: the energy (rapidity) dependence of the scattering amplitude. One can see that the exact solution approaches the asymptotic solution as has been foreseen in the approximate solutions to the problem (see, for example, Refs. [41, 40, 13]).

This result eliminates the last uncertainty that the high energy limit of the scattering amplitude does not show the black disc behaviour but we have rather gray disc one as has been discussed before in Ref. [13]. It turns out that at $\mathcal{Y} \geq 0.5$ ($Y \geq 12.5$) the difference between the exact solution and the asymptotic one is very small. However, for $\mathcal{Y} \leq 0.5$ the difference between the semi-classical approach and the exact solution is rather large and all approximate methods should be taken with the justified suspicion in this kinematic region.

In Appendix D we develop the numerical method specially for small values of Y and we compare it with the exact solution of Eq. (4.10).

6. Comparison with approximate approaches

6.1 Exact solution and the semi-classical approach

As one can see from Fig. 8 the semi-classical approach preserves the singularity structure of the exact solution and correctly reproduces the high energy limit of the amplitude at any value of u but it cannot describe the approaching to this limit. The reason for such a behaviour is clear if we compare the spectrum λ_n at low n of the semi-classical approach given by Eq. (3.22) with the values of λ_n of the exact solution (see Table 1). In the semi-classical solution at small values of n $\Delta\lambda_n = \lambda_{n+1} - \lambda_n = \kappa$ while in the exact spectrum $\Delta\lambda_n < \kappa$.

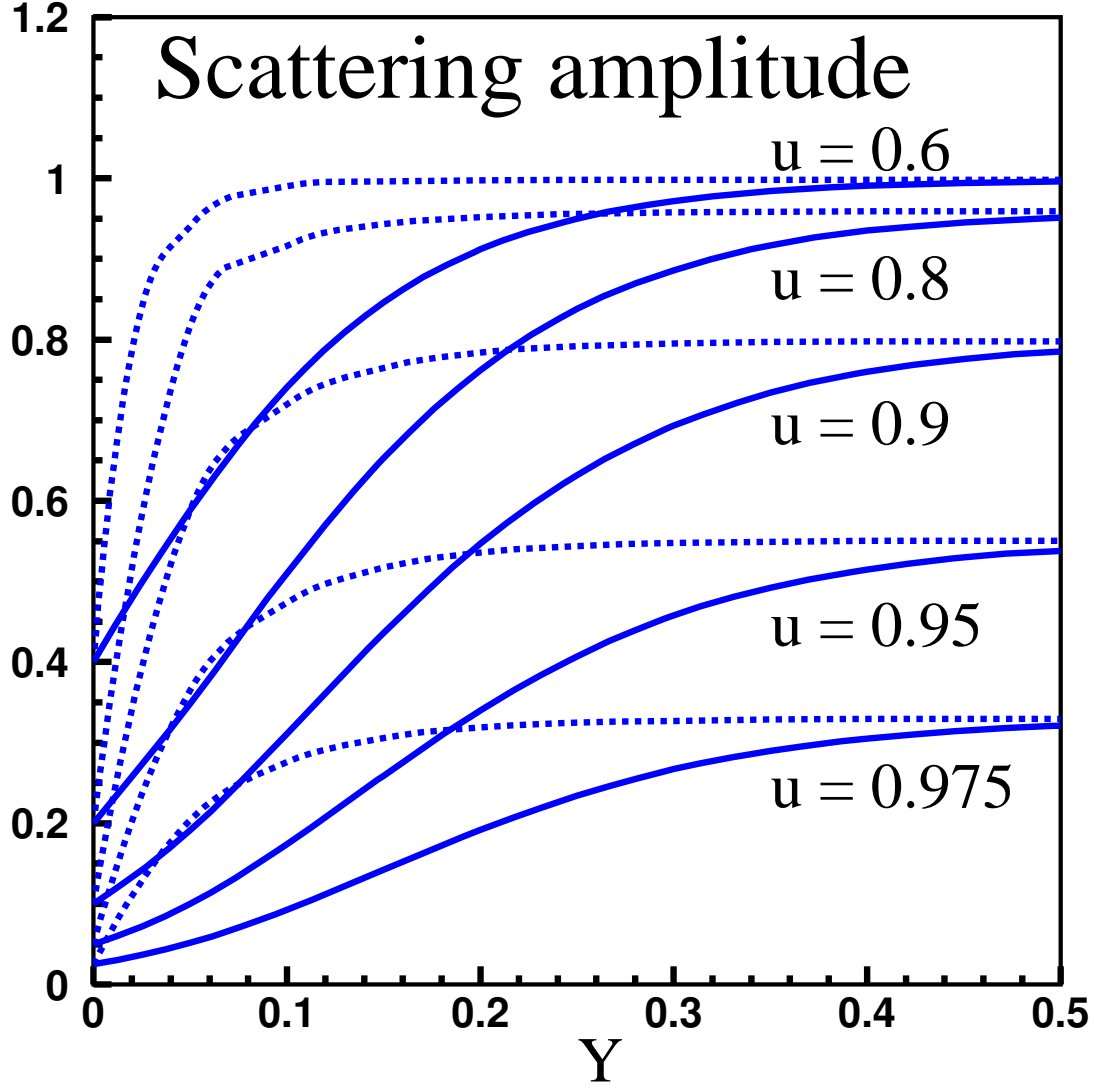


Figure 8: The rapidity dependence of the scattering amplitude $N(Y, u)$ at different values of u . The dashed curves are the semi-classical solution of Eq. (3.26), while the solid lines are the exact solution to the master equation. In this figure we plot $Y \equiv \mathcal{Y}$ (see Eq. (2.2)) and $\kappa = 16$.

6.2 Exact solution and the mean field approximation (MFA)

For the mean field approximation we need to neglect in Eq. (2.1) the second term in the r.h.s. of the

The solution is very simple (see Refs.[9, 10]), namely

$$Z(Y;u) = \frac{u e^{-\kappa Y}}{1 + u (e^{-\kappa Y} - 1)} \quad (6.1)$$

In Fig. 9 we plot the exact solution (solid lines) and the mean field approximation (see Eq. (6.1)).

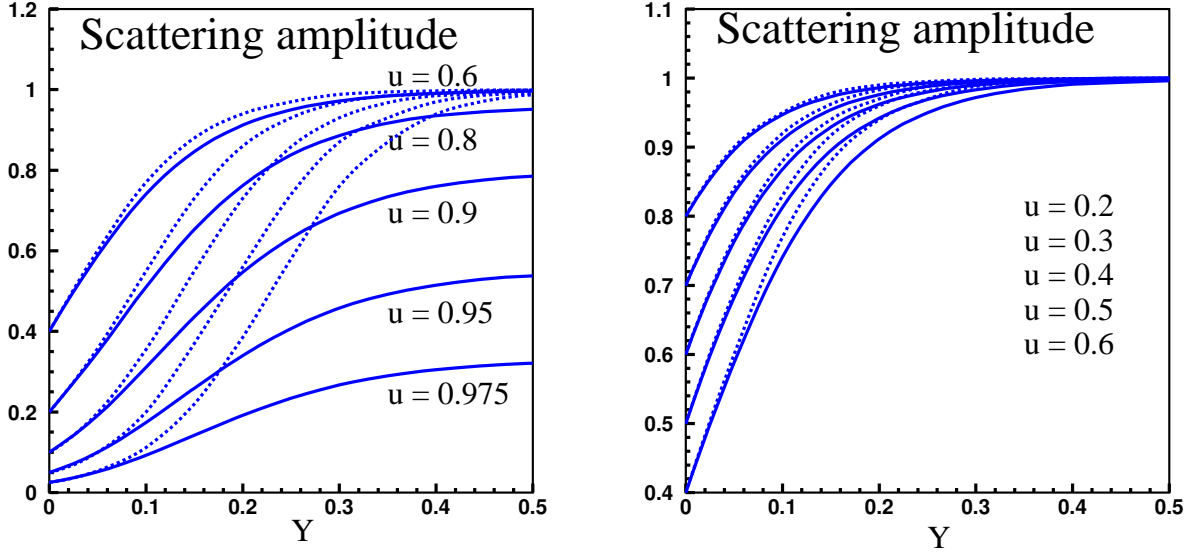


Figure 9: The rapidity dependence of the scattering amplitude $N(Y, u)$ at different values of u . The dashed curves are the mean field approximation given by of Eq. (6.1), while the solid lines are the exact solution to the master equation. In this figure we plot $Y \equiv \mathcal{Y}$ (see Eq. (2.2)) and $\kappa = 16$.

One can see that the mean field approximation cannot describe the scattering amplitude for values of u close to 1, but it gives a good approximation in the region of $u \leq 0.6$ in the wide energy range. However, even for large values of u the MFA fails to reproduce a correct approaching the scattering amplitude to the asymptotic limit.

The physical reason for such a behaviour is clear. The typical value for the scattering amplitude at low energy $\gamma = 1 - u \approx 1/\kappa \leq 1$ for the dipole-dipole scattering. Therefore for the dipole-dipole scattering the exact solution leads to a different behaviour than the mean field approximation. However, if we have the interaction of dipole but with the nucleus target the amplitude at low energies is proportional to $A^{\frac{1}{3}} \gamma(\text{dipole} - \text{dipole}) = A^{\frac{1}{3}}/\kappa = 1 - u \approx 1$ (see for example the paper of Kovchegov in Ref. [17]). The second case when the mean field approximation can work is the deep inelastic scattering. Indeed, we can model this process assuming that $\kappa = 1/\alpha_S^2(Q_s^2)$. However, the scattering amplitude for low energies is proportional to $\alpha_S^2(1/R^2)$ where R is the target size. Therefore, for the running QCD coupling we can assume that $1 - u = \gamma = \alpha_S^2(1/R^2) \approx 1 \geq 1/\kappa$. and the mean field approximation can describe the deep inelastic processes [1].

6.3 Exact solution and the Mueller-Patel-Salam -Iancu (MPSI) approximation.

It was shown by Mueller and Patel[27] (see also Refs. [36, 28, 29, 45]) that in a restricted region of energies we can consider the Pomeron loops larger than $Y/2$. Such loops we can sum and the answer for our model in our notation looks as follows (see Ref. [45])

$$N(Y, u) = 1 - \frac{1}{(1-u) e^{\kappa Y}} \exp \left(\frac{1}{(1-u) e^{\kappa Y}} \right) \Gamma \left(0, \frac{1}{(1-u) e^{\kappa Y}} \right) \quad (6.2)$$

Fig. 10 shows the comparison of the solution given by Eq. (6.2) (dotted lines) with the exact solution (solid lines). One can see that only in the very limited range of energies $Y \leq 0.1$ and at small values of u the MPSI approximation can describe the scattering amplitude.

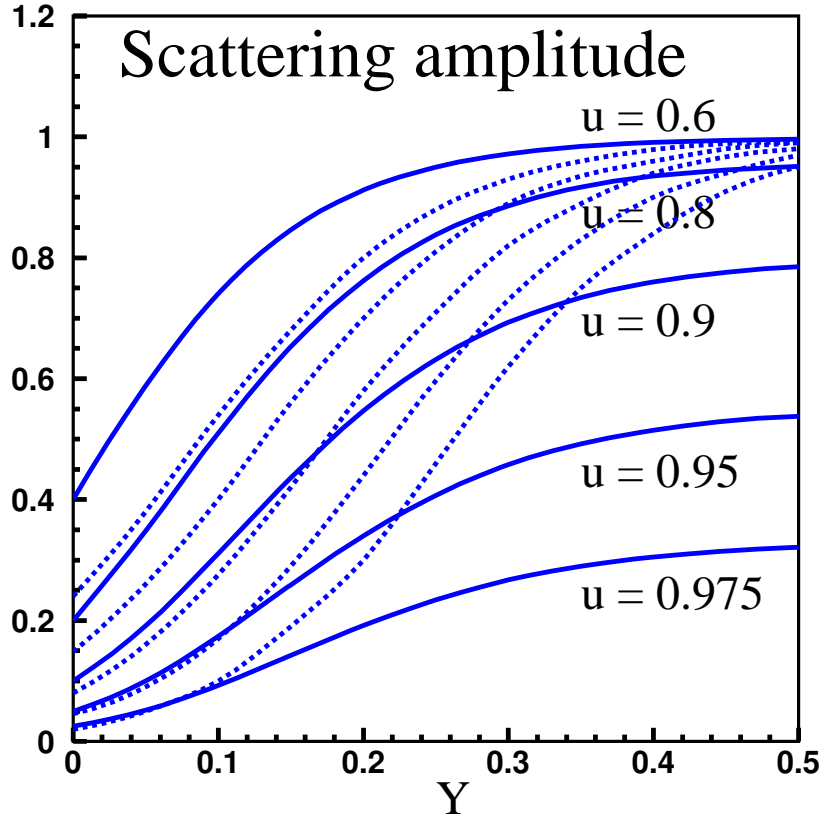


Figure 10: The rapidity dependence of the scattering amplitude $N(Y, u)$ at different values of u . The dashed curves are the MPSI approximation given by of Eq. (6.2), while the solid lines are the exact solution to the master equation. In this figure we plot $Y \equiv \mathcal{Y}$ (see Eq. (2.2)) and $\kappa = 16$.

6.4 Exact solution and the gray disc behaviour.

One of the most interesting results of this paper is the asymptotic gray disc behaviour at ultra high energies: the solution does not go to 1 but to a constant which is smaller than 1 and which depends on the initial conditions or, in other words, on the value of the scattering amplitude at low energies. Such a solution does not contradict to the unitarity constraints and it is consistent with some of the previous approaches (see Refs. [41, 13]). However, among the approximate approaches to the solution of the master equation situations is quite different: most of them: the mean field approximation, the MPSI solution as well as the solution of Ref. [15] lead to the black disc behaviour and only the semi-classical approach gives a constant limit at high energy that is less than 1. Therefore it is worthwhile to discuss the gray disc limit in more details.

The scattering amplitude is equal to [17, 11]

$$\begin{aligned}
N(Y, \gamma(Y_0)) &= 1 - Z(Y, 1 - \gamma(Y_0)) = \sum_{k=1}^{\infty} (-1)^k \gamma^k(Y_0) \left(\sum_{n=1}^{\infty} P_n(Y) \frac{n!}{k!(n-k)!} \right) \\
&\xrightarrow{\gamma(Y_0) \ll 1} \gamma(Y_0) \sum_{n=1}^{\infty} n P_n(Y) = \langle |n| \rangle \times \gamma(Y_0)
\end{aligned} \tag{6.3}$$

where $\gamma(Y_0)$ is the scattering amplitude of one dipole with the target at low energy. If this amplitude is very small Eq. (6.3) shows that the scattering amplitude for the dipole - target scattering at high energy is equal to the product of the low energy amplitude by the average nuenergy ($\langle |n| \rangle$) of dipoles at low energy. Therefore, to obtain the amplitude that equals to 1 at high energy we need to assume that $\langle |n| \rangle$ becomes large (at least of the order of $1/\gamma(Y_0)$). Large number of low energy dipoles is natural to expect in the mean field approximation where the tree ('fan') diagrams contribute (see Fig. 1). On the other hand the mean field approximation violates the t -channel unitarity or, in other words, it gives an incorrect normalization of the parton wave function (see Ref. [46]). Therefore, in the correct answer we rather expect that the average number of partions should be of the order of 1. Indeed, the enhanced diagrams of Fig. 1 are the most essential at high energies to protect the t -channel unitarity [8]. In these diagrams we expect the average number of dipoles at low energy to be the same as in our initial condition, namely, $\langle |n| \rangle \approx 1$. In this situation the behaviour of the amplitude at high energies depends on the value of the scattering amplitude at low energies as we see in our exact solution.

This result we could also foresee if we considered the first corrections to the vertex of splitting of one Pomeron to two Pomerons (transition $P \rightarrow 2P$, see Fig. 11). First thing that we can see from this picture, which graphically shows the result of integration with respect to y_2 , that the first corrections lead to an increase of the value of the $2P \rightarrow P$ vertices with rapidities y_1 (the first diagram in Fig. 11) and y (the second diagram in Fig. 11). Indeed, the simple diagram in Fig. 11 has the following explicit expression

$$\begin{aligned}
A(\text{Fig. 11}) &= \Gamma^2(1 \rightarrow 2) \Gamma(2 \rightarrow 1) \int_y^Y dy_1 \int_0^y dy_2 e^{\Gamma(1 \rightarrow 2)(Y+y_1+y-y_2)} \\
&= \Gamma(1 \rightarrow 2) \Gamma(2 \rightarrow 1) \int_y^Y dy_1 \left\{ e^{\Gamma(1 \rightarrow 2)(Y+y_1)} - e^{\Gamma(1 \rightarrow 2)(Y+y_1+y)} \right\}
\end{aligned} \tag{6.4}$$

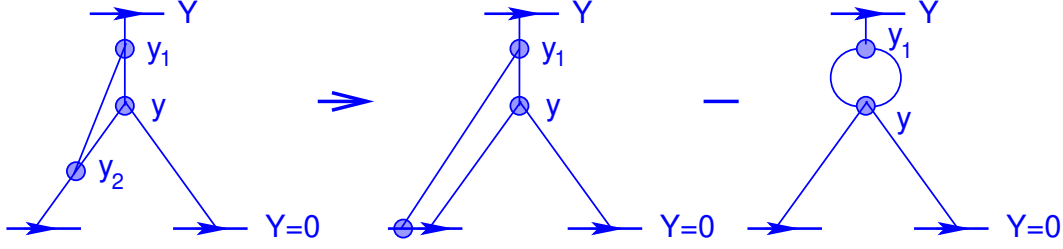


Figure 11: The first correction to the $P \rightarrow 2P$ vertex due to the merging of two Pomerons into one Pomeron. Solid lines are Pomerons. Lines with arrows denote the interacting dipoles.

Having this observation in mind we solve the mean field equations but assuming that the vertex for $P \rightarrow P$ transition (Δ) is not equal to the vertex of splitting of one Pomeron to two Pomerons $\Gamma(1 \rightarrow 2)$. The equation has the form

$$\frac{\partial Z(Y; u)}{\partial Y} = (-\Delta u + \Gamma(1 \rightarrow 2) u^2) \frac{\partial Z(Y; u)}{\partial u} \quad (6.5)$$

Eq. (6.5) has an obvious solution, which for the scattering amplitude has the form

$$N(Y, \gamma(Y_0)) = \frac{\gamma(Y_0) e^{\Delta(Y-Y_0)}}{1 + \gamma(Y_0) \Gamma(1 \rightarrow 2) (e^{\Delta(Y-Y_0)} - 1)} \xrightarrow{Y-Y_0 \gg 1} \frac{\Delta}{\Gamma(1 \rightarrow 2)} \quad (6.6)$$

One can see that if $\Gamma(1 \rightarrow 2) > \Delta$ we expect a gray disc. It is easy to check that the MPSI approximation with different vertices for $P \rightarrow P$ and $P \rightarrow 2P$ transitions give the same answer as Eq. (6.6). Therefore, Eq. (6.4) shows that the gray disc behaviour is very likely for the exact solution.

Formally speaking we expect to have two asymptotic solutions (Z_∞) which stem from the master equation with $\partial Z_\infty / \partial Y = 0$, since the equation is the second order differential equation. The linear combination which satisfy the boundary conditions $Z_\infty(u = 0) = 0$ and $Z_\infty(u = 1) = 1$, is the solution to the problem at high energy, which leads to a gray disc behaviour of the scattering amplitude. These two boundary conditions are very natural since they say: (i) for $u = 0$, that if amplitude is equal to 1 at $Y = 0$ none of interactions can change this fact due to the s -channel unitarity; and (ii) for $u = 1$, that starting with zero amplitude for dipole interaction at $Y = 0$, we cannot obtain an amplitude different from zero in an interacting system. Therefore, neither the fact of two asymptotic solutions nor the boundary conditions depend on the particular form of interaction. For example, they do not depend on whether we took into account the possibility for two Pomerons to re-scatter in two Pomerons as it is done in this paper, or whether we neglect such interaction as was assumed in Ref. [15]. In both cases we have the asymptotic solution, that satisfies the boundary conditions of the gray disc. One of the main result of this paper is the proof that nothing unusual happens with the system in the process of evolution from $Y = 0$ to very large values of Y and the resulting solution approaches the asymptotic one. To understand this result it is instructive to share with our reader what kind of an alternative solution we could expect. Frankly speaking, we can expect in such kind of problem the asymptotic solution that has a singularity in the singular points of this equation ($u = 0$ and $u = 1$). Even more, the solution of the mean field

approximation, for which we have the same boundary condition, has an asymptotic solution, which we can write in the form

$$Z_{\infty}(u) = \Theta(1 - u) \quad (6.7)$$

One can see that $Z_{\infty}(u) = 0$ for $u < 1$ and $Z_{\infty}(u) = 1$ for $u = 1$. However, this solution has an singular behaviour and $Z'_u = \delta(1 - u)$. Nevertheless, since $(1 - u)\delta(1 - u) = 0$ this is a solution. The solution that we found shows that in general case there is no such singular solution. Of course, the last claim is based on our believe that the physical problem has one and the only one solution. One can check that $(1 - u)(d^2\Theta(1 - u)/d^2u) \rightarrow i\infty$ at $u \rightarrow 1$.

Our conclusion is very simple: the asymptotic behaviour of the exact solution is not only the gray disc but this kind of behaviour gives us a check how well an approximate method is able to discuss the high energy scattering. However, it should be very carefully stated that the real QCD case can be different; and we have arguments for both scenarios: black disc behaviour [47, 48] and the gray disc one [13]. The difference is in the extra integration over sizes of produced dipoles. The scattering amplitude in the Born approximation of perturbative QCD is very large for the dipoles of the large sizes. Therefore, the equation of Eq. (6.3) - type can give the black disc even if the average number of dipoles is about 1 since it can be one dipole but of very large size. However, the question, whether we can trust the perturbative QCD calculations for such dipoles, is the open question.

7. Conclusions

The core of this paper is the exact analytical solution to the BFKL Pomeron calculus in the zero transverse dimension given in section 4. The method, that we proposed, is very general and can be applied to a various kind of practical problems in future.

The scattering amplitude at high energies, which stems from the exact solution, shows the gray disc behaviour of the asymptotic solution (see Eq. (2.43)). Therefore, we filled the hole in the proof demonstrating that the asymptotic behaviour of Eq. (2.43) satisfies the initial conditions.

We found thainitialapproximations to the master equation, developed in the past (see Refs. [41, 40, 13, 14, 15]), work quite well at large values of rapidity ($Y \geq 10$) and can be used in either asymptotic estimates or for an illustration of the main properties of the high energy interaction. The advantage of all of them is their simplicity and transparent physics ideas that are behind these methods. In this respect the semi-classical approach is especially attractive since it gives the clear understanding of the spectrum of the problem and the behaviour of the eigenfunctions. However, the comparison with the exact solution shows that we cannot trust the approximate methods for low energies, namely, for $Y \leq 10$ where there exist the most of the experimental data including ones that we anticipate from the LHC.

We firmly believe that the solution for the BFKL Pomeron calculus at zero transverse dimension is the necessary step in our understanding of the behaviour of the scattering amplitude at high energies in QCD. The real QCD problem is much more complicated but the fact, that we can compare the approximation methods with the exact solution for our toy model and found how they work, might open a way to solve

the QCD problem at high energies developing different approximations (see Refs.[27, 28, 29, 13] where one can see the first attempts of such kind of approaches).

Acknowledgments:

We want to thank Asher Gotsman, Edmond Iancu, Volodya Khachtryan, Uri Maor and Jeremy Miller for very useful discussions on the subject of this paper. The special thanks go to Bo-Wen Xiao for discussion with us the results of Ref. [15].

This research was supported in part by the Israel Science Foundation, founded by the Israeli Academy of Science and Humanities and by BSF grant # 20004019.

A. Appendix A: General way for solving linear nonhomogeneous boundary problem.

At this appendix we describe the general way for solving linear non-homogeneous boundary value problem using the appropriate Green's functions, that can be constructed from the eigenfunctions of the Sturm-Liouville problem.

Here we are dealing only with the issues related to solutions of the master equation, which is equivalent to the BFKL Pomeron calculus in zero transverse dimension, while for more detail information, related to this subject, one can find in Ref. [22].

First of all, it is easily to check this using trivial transformations:

$$\begin{aligned} s(v) &= \frac{1}{f(v)} \exp \left[\int \frac{g(v)}{f(v)} dv \right], \quad p(v) = \exp \left[\int \frac{g(v)}{f(v)} dv \right], \\ q(v) &= -\frac{h(v)}{f(v)} \exp \left[\int \frac{g(v)}{f(v)} dv \right] \end{aligned} \quad (\text{A.1})$$

the general linear non-homogeneous partial differential equation of the parabolic type:

$$\frac{\partial Z}{\partial y} = f(v) \frac{\partial^2 Z}{\partial v^2} + g(v) \frac{\partial Z}{\partial v} + h(v)Z + \varphi(y, v) \quad (\text{A.2})$$

can be reduced to the equation which is suitable finding a solution to the Sturm-Liouville problem:

$$s(v) \frac{\partial Z}{\partial y} = \frac{\partial}{\partial v} \left[p(v) \frac{\partial Z}{\partial v} \right] - q(v)Z + s(v)\varphi(y, v) \quad (\text{A.3})$$

Denoting by $\Phi(y, v) = s(v)\varphi(y, v)$ we have the equation:

$$s(v) \frac{\partial Z}{\partial y} = \frac{\partial}{\partial v} \left[p(v) \frac{\partial Z}{\partial v} \right] - q(v)Z + \Phi(y, v) \quad (\text{A.4})$$

For arbitrary initial $Z(0, v) = \theta(v)$ and boundary $Z(y, v_1) = \alpha$, $Z(y, v_2) = \beta$ conditions the general solution is given by the following expression (see Refs. [21, 22]):

$$\begin{aligned} Z(y, v) = & \int_0^y \int_{v_1}^{v_2} \Phi(\tau, \xi) \cdot G(y - \tau, v, \xi) d\tau d\xi + \int_{v_1}^{v_2} s(\xi) \cdot \theta(\xi) \cdot G(y, v, \xi) d\xi \\ & + p(v_1) \int_0^y \alpha \cdot \Lambda_1(y - \tau, v) d\tau + p(v_2) \int_0^y \beta \cdot \Lambda_2(y - \tau, v) d\tau \end{aligned} \quad (\text{A.5})$$

Here the Green's function is given by:

$$G(y, v, \xi) = \sum_{n=1}^{\infty} \frac{Z_n(v) Z_n(\xi)}{\|Z_n\|^2} \exp(-\lambda_n y) ; \quad \|Z_n\|^2 = \int_{v_1}^{v_2} s(v) \cdot Z_n^2(v) dv ; \quad (\text{A.6})$$

where the λ_n and $Z_n(v)$ are the eigenvalues and corresponding eigenfunctions of the following Sturm-Liouville problem for the second order linear differential equation:

$$(p(v)\tilde{Z}')' + [\lambda s(v) - q(v)]\tilde{Z} = 0 \quad (\text{A.7})$$

with the boundary conditions

$$\tilde{Z}(v_1) = \alpha, \quad \tilde{Z}(v_2) = \beta. \quad (\text{A.8})$$

The functions Λ_1 Λ_2 are expressed via the Green's function:

$$\Lambda_1(y, v) \equiv \lim_{\xi \rightarrow v_1} \frac{\partial}{\partial \xi} G(y, v, \xi) ; \quad \Lambda_2(y, v) \equiv \lim_{\xi \rightarrow v_2} \frac{\partial}{\partial \xi} G(y, v, \xi) . \quad (\text{A.9})$$

The most complicated part in Eq. (A.5) is the two last terms that include functions Λ_1 , Λ_2 and require applying of some regularization technique in calculating them. Fortunately, we can find a simple transformation after which these two terms will disappear. Namely, subtracting from $Z(y, v)$ the initial conditions:

$$\tilde{Z}(y, v) = Z(y, v) - Z(0, v) \quad (\text{A.10})$$

we will obviously have equation for function $\tilde{Z}(y, v)$ with zero boundary conditions:

$$\tilde{Z}(y, v_1) = \tilde{Z}(y, v_2) = 0 \quad (\text{A.11})$$

and zero initial conditions:

$$\tilde{Z}(0, v) = 0. \quad (\text{A.12})$$

The only price for this transformation is transformation of the free term in Eq. (A.4):

$$\tilde{\Phi}(y, v) = \Phi(y, v) + \frac{\partial}{\partial v} \left[p(v) \frac{\partial Z(0, v)}{\partial v} \right] - q(v) Z(0, v) \quad (\text{A.13})$$

Thus we have only the first term (term which has nonzero contribution) in Eq. (A.5) for the function $\tilde{Z}(y, v)$:

$$\tilde{Z}(y, v) = \int_0^y \int_{v_1}^{v_2} \tilde{\Phi}(\tau, \xi) \cdot G(y - \tau, v, \xi) d\tau d\xi \quad (\text{A.14})$$

and final answer obviously has the following form:

$$Z(y, v) = Z(0, v) + \tilde{Z}(y, v) = Z(0, v) + \int_0^y \int_{v_1}^{v_2} \tilde{\Phi}(\tau, \xi) \cdot G(y - \tau, v, \xi) d\tau d\xi \quad (\text{A.15})$$

Note, that using Eq. (A.15) we reduce Eq. (A.3) to the equation for $\tilde{Z}(y, v)$ which has the same form as Eq. (A.4) but with the inhomogeneous term $\tilde{\Phi}(y, v)$ given by Eq. (A.13). The advantage of this transform is clear if we compare the rather compact answer of Eq. (A.15) with the solution in the form of Eq. (A.5).

B. Appendix B: The exact semi-classical solution.

At this appendix we calculate exactly functions $\phi^\pm(\omega, u)$ for the semi-classical solution (see section 3.1) and compare them with the approximations at small and large values of ω , which were used for calculation in this section.

Recall that

$$\frac{d\phi^\pm}{du} = \frac{\kappa}{2} \left\{ 1 \pm \sqrt{1 + \frac{4\omega}{\kappa^2 u(1-u)}} \right\} \quad (\text{B.1})$$

Therefore, functions ϕ^\pm (see Eq. (3.1) and Eq. (3.4)) are defined by the following integrals:

$$\phi^\pm(u) = - \int_u^1 \frac{\kappa}{2} \left\{ 1 \pm \sqrt{1 + \frac{4\omega}{\kappa^2 u'(1-u')}} \right\} du' = I_1 + I_2 \quad (\text{B.2})$$

where the first integral is trivial:

$$I_1 = - \int_u^1 \frac{\kappa}{2} du' = \frac{\kappa}{2} (u - 1) \quad (\text{B.3})$$

The second term ⁷ is a bit more complicated and can be expressed using well known elliptic integrals:

$$\begin{aligned} I_2 &= \mp \frac{\kappa}{2} \int_u^1 \sqrt{1 + \frac{4\omega}{\kappa^2 u'(1-u')}} du' \\ &= \mp \frac{\kappa}{2} \sqrt{\frac{1}{4} + \frac{4\omega}{\kappa^2}} \left[EE \left(\frac{\pi}{2}, \frac{1}{1 + 16\omega/\kappa^2} \right) + EE \left(\text{ArcSin}[1 - 2u], \frac{1}{1 + 16\omega/\kappa^2} \right) \right] \end{aligned} \quad (\text{B.4})$$

⁷We very grateful to our referee, who noticed that I_2 can be reduced to this relatively simple form.

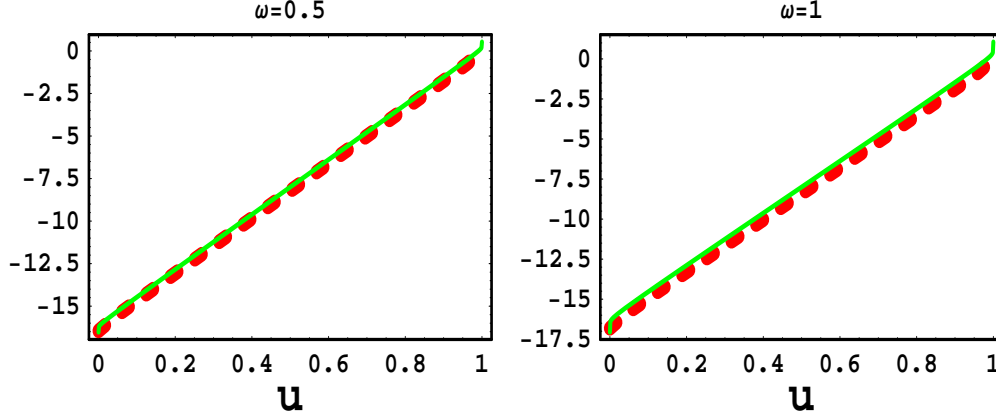


Figure 12: This plot shows the exact function $\phi^+(\omega, u)$ (thick dotted line) and the approximate function $\phi(\omega)$ of Eq. (3.6) (thin solid line) for small values of ω (i.e. $\omega \leq \kappa^2$). $\kappa = 16$ for the plot.

Where $EE(\varphi, m)$ is the elliptic integral of the second kind [24]

$$EE(\varphi, m) \equiv \int_0^\varphi (1 - m \cdot \sin^2(\theta))^{+1/2} d\theta \quad (\text{B.5})$$

We can see that, in spite the fact that ϕ^\pm can be calculated explicitly (in radicals), the received expression is too complicated in order to use it for the calculations of the functions $\Phi^\pm(\omega)$ in Eq. (3.5). Nevertheless, this exact calculation is very useful by two reasons: (i) using exact form of ϕ^\pm we can estimate the accuracy of our approximate expression for functions $\phi^\pm(\omega, u)$, and (ii) we can find the separation parameter between small and large ω that we used in our semi-classical solution of section 3.2.

The plots in Fig. 12 and in Fig. 13 illustrate how good our approach for small and large ω , which we used for calculations of ϕ^\pm .

C. Appendix C: Hermitian Hamiltonian description of rapidity evolution in zero transverse dimensions

At this appendix we give the answer to the important question: whether rapidity evolution in zero transverse dimensions can be described by hermitian Hamiltonian? Or, in other words: do we have probability conservation in these processes?

First of all, let us rewrite our master equation Eq. (2.1):

$$\frac{\partial Z}{\partial y} = u(1-u) \left(-\kappa \frac{\partial Z}{\partial u} + \frac{\partial^2 Z}{\partial u^2} \right) \quad (\text{C.1})$$

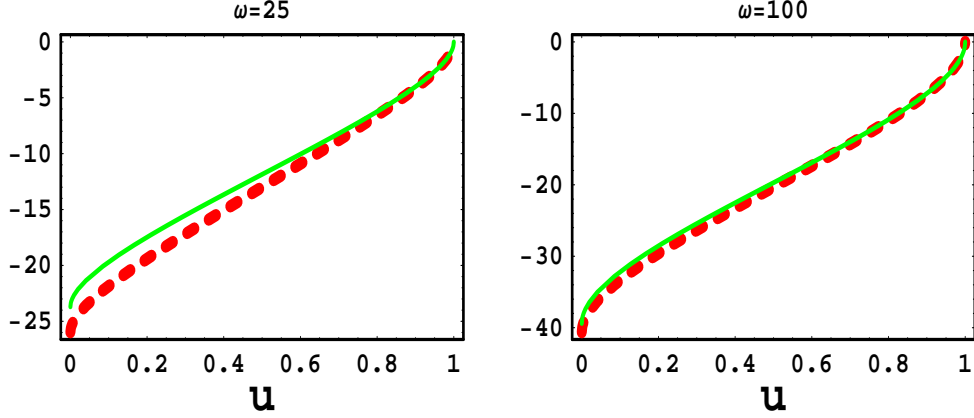


Figure 13: This plot shows the exact function $\phi^+(\omega, u)$ (thick dotted line) and the approximate function $\phi(\omega)$ of Eq. (3.6) (thin solid line) for large values of ω (i.e. $\omega \geq \kappa^2$). $\kappa = 16$ for the plot.

in the form of the Fokker-Plank equation, using the simple transformation: $Z(y, u) = u(1 - u) \cdot \tilde{Z}(y, u)$

$$\frac{\partial \tilde{Z}}{\partial y} = - \frac{\partial}{\partial u} \left(\kappa u(1 - u) \cdot \tilde{Z}(y, u) \right) + \frac{\partial^2}{\partial u^2} \left(u(1 - u) \cdot \tilde{Z}(y, u) \right) \quad (\text{C.2})$$

It is natural to define the Fokker-Plank operator as

$$\hat{L}_{FP} \equiv - \frac{\partial}{\partial u} a(u) + \frac{\partial^2}{\partial u^2} b(u) \quad (\text{C.3})$$

where in our case $a(u) = \kappa u(1 - u)$ and $b(u) = u(1 - u)$. Introducing potential $\Phi(u)$ such that:

$$\Phi(u) \equiv \ln[b(u)] - \int_{u_1}^u \frac{a(u')}{b(u')} du' = \ln[u(1 - u)] - \kappa \quad (\text{C.4})$$

we can rewrite \hat{L}_{FP} in the following form:

$$\hat{L}_{FP} = \frac{\partial}{\partial u} b(u) e^{-\Phi(u)} \frac{\partial}{\partial u} e^{\Phi(u)} \quad (\text{C.5})$$

Now it is obviously that \hat{L}_{FP} is non-hermitian operator. Nevertheless, operator $\hat{L}_H = e^{\Phi(u)/2} \hat{L}_{FP} e^{-\Phi(u)/2}$ is hermitian (in some sense we restored the hermitian property of our system). Indeed we can check this by the direct calculation:

$$\int_{u_1}^{u_2} \phi_1(u) e^{\Phi(u)} \hat{L}_{FP} \phi_2(u) du = \int_{u_1}^{u_2} \phi_1(u) e^{\Phi(u)} \frac{\partial}{\partial u} b(u) e^{-\Phi(u)} \frac{\partial}{\partial u} e^{\Phi(u)} \phi_2(u) du$$

$$\begin{aligned}
&= - \int_{u_1}^{u_2} \left[\frac{\partial}{\partial u} \phi_1(u) e^{\Phi(u)} \right] b(u) e^{-\Phi(u)} \left[\frac{\partial}{\partial u} \phi_2(u) e^{\Phi(u)} \right] du \\
&= \int_{u_1}^{u_2} \phi_2(u) e^{\Phi(u)} \frac{\partial}{\partial u} b(u) e^{-\Phi(u)} \frac{\partial}{\partial u} e^{\Phi(u)} \phi_1(u) du \\
&= \int_{u_1}^{u_2} \phi_2(u) e^{\Phi(u)} \hat{L}_{FP} \phi_1(u) du
\end{aligned} \tag{C.6}$$

where $\phi_1(u)$ and $\phi_2(u)$ are two functions, which satisfy boundary conditions. Therefore, we have demonstrated that $\left(e^{\Phi(u)} \hat{L}_{FP} \right)^\dagger = \hat{L}_{FP}^\dagger e^{\Phi(u)} = e^{\Phi(u)} \hat{L}_{FP}$

It is important to note that transformation $\hat{L}_H = e^{\Phi(u)/2} \hat{L}_{FP} e^{-\Phi(u)/2}$ can be alternatively considered as a transformation of the appropriate eigenfunctions. If $\phi_n(u)$ are the eigenfunctions of the Fokker-Planck operator \hat{L}_{FP} with the eigenvalues λ_n , the $\psi_n(u) = e^{\Phi(u)/2} \phi_n(u)$ will be the eigenfunctions of operator \hat{L}_H with the same eigenvalues. Actually, appropriate transformation of eigenfunctions was used in our paper in order to restore Hermitian property of our system.

It is obviously that both of system $\phi_n(u)$ and $\psi_n(u)$ predefine the orthogonal and complete systems:

- Orthogonality:
 $\int_{u_1}^{u_2} e^{\Phi(u)} \phi_n(u) \cdot \phi_m(u) du = \int_{u_1}^{u_2} \psi_n(u) \cdot \psi_m(u) du = \delta_{nm}$
- Completeness:
 $e^{\Phi(u)} \sum_n \phi_n(u) \cdot \phi_n(u') = \sum_n \psi_n(u) \cdot \psi_n(u') = \delta(u - u')$

D. Appendix D: The exact solution as a power series in rapidity

Our master equation Eq. (2.1) can be solved exactly for the arbitrary initial conditions: $Z(Y = 0; u) = f(u)$ in terms of the power series of rapidity. This method has a number of exclusive advantages: (I) it applicable for all reasonable initial conditions, which allow us to apply such solution for the different scattering processes at high energies; (II) with this method we can easily solve all modifications of our master equation, which incorporates next order corrections with the only one restriction that the variable coefficients in the diffusion equation can be represented as power series in u ; (III) this method extremely good for small values of rapidity y and in vicinity of $u = 0$ and $u = 1$ (we will demonstrate this below with numerical calculations). The last argument especially important, since all solutions, which are based on approximate methods, lead to large errors just for small values of rapidity y and/or in vicinity of $u = 0$ and $u = 1$.

Unfortunately, solution in terms of power series of rapidity is converged relatively slowly, thus this method is not applicable for calculations of the asymptotic behaviors of the scattering amplitude. Nevertheless, we believe that proposed method will be very useful for practical calculations, because most of the experimental data, available now, are concentrated at small or intermediate values of rapidity.

It is very instructive to start with the direct decompositions of function $Z(\mathcal{Y}, u)$:

$$Z(\mathcal{Y}, u) = \sum_{n=0}^{\infty} C_n(u) \cdot \mathcal{Y}^n \quad (\text{D.1})$$

It is obviously the first term in such expansion corresponds to appropriate initial conditions, indeed at $\mathcal{Y} = 0$ we have:

$$Z(\mathcal{Y} = 0, u) = \sum_{n=0}^{\infty} C_n(u) \cdot (\mathcal{Y} = 0)^n = C_0(u) = f(u) \quad (\text{D.2})$$

Now by substitution of Eq. (D.1) into our master equation Eq. (2.1) and after arranging the appropriate powers of \mathcal{Y} we will get the following recurrence equations for the functions $C_n(u)$:

$$C_{n+1}(u) = \frac{u(1-u)}{n+1} \cdot \left[\frac{\partial^2 C_n(u)}{\partial u^2} - \kappa \frac{\partial C_n(u)}{\partial u} \right] \quad (\text{D.3})$$

Therefore, once we know initial conditions of our problem Eq. (D.2), all series expansions Eq. (D.1) are well defined and can be calculated up to arbitrary order. Finally, introducing the differential operator \hat{L}^n as follows

$$\hat{L}^i[f(u)] \equiv \hat{L} \left[\hat{L}^{i-1}[f(u)] \right] ; \quad \hat{L} \equiv \frac{u(1-u)}{n+1} \cdot \left[\frac{\partial^2}{\partial u^2} - \kappa \frac{\partial}{\partial u} \right] \quad (\text{D.4})$$

the answer can be written in the very elegant form:

$$Z(\mathcal{Y}, u) = f(u) + \sum_{n=1}^{\infty} \hat{L}^n[f(u)] \cdot \mathcal{Y}^n \quad (\text{D.5})$$

This result is nice from the analytical point of view: (1) it haven't singularities, (2) the expansion is well defined for all orders. Nevertheless, for numerical estimations probably not so usefully. The reason for this is clear: series expansion Eq. (D.5) is converged relatively slowly and even more, the radius of convergence is the function of u . For example, taking first 20 terms of our expansion we can ensure solution $Z(\mathcal{Y}, u)$ in rapidity rang $Y \in [0, 5]$. So from numerical point of view this solution can be considered as solution for small and intermediate values of rapidity.

Fortunately, we can improve numerical property of proposed solution by simple modification, namely we are going expand not the function $Z(\mathcal{Y}, u)$, but function $\varphi(\mathcal{Y}, u) = \ln[Z(\mathcal{Y}, u)]$. It is obviously that this modification was inspired by our experience in semi-classical solution, but now we are going to keep all terms and propose exact solution.

The first step, which we do is rewriting our master equation Eq. (2.1) in terms of function $\varphi(\mathcal{Y}, u) = \ln[Z(\mathcal{Y}, u)]$, by simple substitution we get the following equation for $\varphi(\mathcal{Y}, u)$:

$$\frac{\partial \varphi}{\partial \mathcal{Y}} = u(1-u) \cdot \left(\left(\frac{\partial \varphi}{\partial u} \right)^2 + \frac{\partial^2 \varphi}{\partial u^2} - \kappa \frac{\partial \varphi}{\partial u} \right) \quad (\text{D.6})$$

Now one again, we search a solution for this equation in terms of power series of rapidity:

$$\varphi(\mathcal{Y}, u) = \sum_{n=0}^{\infty} B_n(u) \cdot \mathcal{Y}^n \quad (\text{D.7})$$

Substituting Eq. (D.7) into Eq. (D.6) and arranging the appropriate powers of \mathcal{Y} , we obtain the following recurrent relations for functions $B_n(u)$:

$$B_{n+1}(u) = \frac{u(1-u)}{n+1} \cdot \left[\sum_{k=0}^n \frac{\partial B_k(u)}{\partial u} \cdot \frac{\partial B_{n-k}(u)}{\partial u} + \frac{\partial^2 B_n(u)}{\partial u^2} - \kappa \frac{\partial B_n(u)}{\partial u} \right] \quad (\text{D.8})$$

The appropriate initial condition for function $\varphi(\mathcal{Y}, u)$ is also simple in transformation:

$$\varphi(\mathcal{Y} = 0, u) = \sum_{n=0}^{\infty} B_n(u) \cdot (\mathcal{Y} = 0)^n = B_0(u) = \ln[f(u)] \quad (\text{D.9})$$

The last solution numerically is much more stable and, taking first 20 terms of our expansion, we can ensure solution $Z(Y, u)$ already in rapidity rang $Y \in [0, 8]$. It is important to note that proposed logarithmic transformation works well in all cases, except the specific initial conditions: $Z(\mathcal{Y} = 0, u) = \text{const}$ (fortunately, for our physical environment such initial conditions does not look reasonable).

Finally, we demonstrate the quality of this method comparing it with the exact solution of Eq. (4.10). It is obviously that for small values of rapidity this method work quite well.

E. Appendix E: The interaction procedure for the spectrum of the problem

In this appendix we show that the iteration procedure that has been described in 2.3, works quite well at least for calculations of the eigenvalues for the master equation (see Eq. (2.1)). Starting with the exact spectrum of the equation at large values of n (see Eq. (2.17)) and using the set of eigenfunctions we can develop the regular perturbative approach based on Eq. (2.44) with $U_0(\Theta)$ being the rectangular-well potential and choosing $V(\Theta) = \frac{\kappa^2}{4} \sin^2 \Theta$. The corrections to the eigenvalues ($\Delta \lambda_n$) are determined by the simple formula

$$\Delta \lambda_n = \int_0^\pi d\Theta V(\Theta) |\Psi(\Theta)|^2 \quad (\text{E.1})$$

and the resulting

$$\lambda_n = n^2 + \Delta \lambda_n \quad (\text{E.2})$$

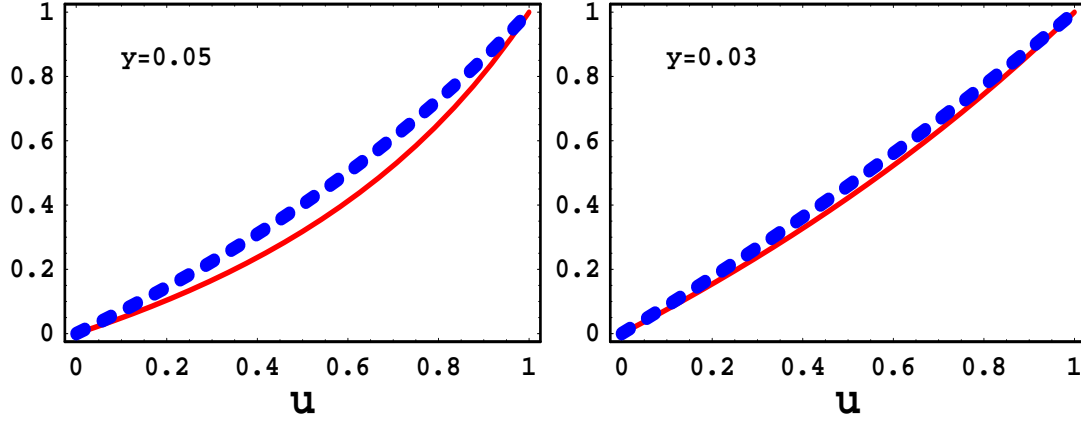


Figure 14: In this plot we compare the exact solution of Eq. (4.10) - a solid line and the solution, given by the power series in rapidity, taking into account first 20 terms (see Eq. (D.5)) - a dashed line. This comparison is performed for two different values of rapidity. As we can see from the plots these solutions are close. In principle, the exact solution is a bit steeper than the power series solution, which obviously reflects the fact that we took into account a limited number of terms in this expansion.

Eigenvalues	λ_1	λ_2	λ_3	λ_4	λ_5	λ_6	λ_7	λ_8	λ_9	λ_{10}
Spheroidal (exact)	13.0	14.13	21.40	28.63	38.45	50.32	64.24	80.19	98.15	118.13
Asymptotic ($\lambda_n = n^2$)	1	4	9	16	25	36	49	64	81	100
First iteration	14.25	14.75	21.25	29.75	40.25	52.75	67.25	83.75	102.25	122.75

Table 1: The comparison of the first ten eigenvalues of the master equation with the asymptotic estimates and with the first iteration described in section 2.3.

One can see from the Table I that this first iteration leads to the eigenvalues which are very close to the exact eigenvalues of the master equation.

From this table we see that the first iteration reproduces correctly the values of the eigenvalues at small n . Therefore, we can conclude that the iteration procedure, described in section 2.3, gives the way to approach the exact solution with a good accuracy.

References

- [1] L. V. Gribov, E. M. Levin and M. G. Ryskin, *Phys. Rep.* **100**, 1 (1983).
- [2] A. H. Mueller and J. Qiu, *Nucl. Phys.*, 427 **B 268** (1986) .
- [3] E. A. Kuraev, L. N. Lipatov, and F. S. Fadin, *Sov. Phys. JETP* **45**, 199 (1977); Ya. Ya. Balitsky and L. N. Lipatov, *Sov. J. Nucl. Phys.* **28**, 22 (1978).
- [4] J. Bartels, M. Braun and G. P. Vacca, *Eur. Phys. J.* **C40**, 419 (2005) [arXiv:hep-ph/0412218]; J. Bartels and C. Ewerz, *JHEP* **9909**, 026 (1999) [arXiv:hep-ph/9908454]; J. Bartels and M. Wusthoff, *Z. Phys.* **C66**, 157 (1995); A. H. Mueller and B. Patel, *Nucl. Phys.* **B425**, 471 (1994) [arXiv:hep-ph/9403256]; J. Bartels, *Z. Phys.* **C60**, 471 (1993).
- [5] M. A. Braun, *Phys. Lett.* **B632** (2006) 297 [arXiv:hep-ph/0512057]; arXiv:hep-ph/0504002; *Eur. Phys. J.* **C16**, 337 (2000) [arXiv:hep-ph/0001268]; M. Braun, *Eur. Phys. J.* **C6**, 321 (1999) [arXiv:hep-ph/9706373]; M. A. Braun and G. P. Vacca, *Eur. Phys. J.* **C6**, 147 (1999) [arXiv:hep-ph/9711486].
- [6] H. Navelet and R. Peschanski, *Nucl. Phys.* **B634**, 291 (2002) [arXiv:hep-ph/0201285]; *Phys. Rev. Lett.* **82**, 137 (1999), [arXiv:hep-ph/9809474]; *Nucl. Phys.* **B507**, 353 (1997) [arXiv:hep-ph/9703238].
- [7] J. Bartels, L. N. Lipatov and G. P. Vacca, *Nucl. Phys.* **B706**, 391 (2005) [arXiv:hep-ph/0404110].
- [8] V. N. Gribov, *Sov. Phys. JETP* **26**, 414 (1968) [*Zh. Eksp. Teor. Fiz.* **53**, 654 (1967)].
- [9] A. H. Mueller, *Nucl. Phys.* **B415**, 373 (1994); *ibid* **B437**, 107 (1995).
- [10] E. Levin and M. Lublinsky, *Nucl. Phys.* **A730**, 191 (2004) [arXiv:hep-ph/0308279].
- [11] E. Levin and M. Lublinsky, *Phys. Lett.* **B607**, 131 (2005) [arXiv:hep-ph/0411121].
- [12] E. Levin and M. Lublinsky, *Nucl. Phys.* **A763**, 172 (2005) , arXiv:hep-ph/0501173.
- [13] E. Levin, *Nucl. Phys.* **A763**, 140 (2005), arXiv:hep-ph/0502243.
- [14] P. Rembiesa and A. M. Stasto, *Nucl. Phys.* **B725** (2005) 251 [arXiv:hep-ph/0503223].
- [15] A. I. Shoshi and B. W. Xiao, “Pomeron loops in zero transverse dimensions,” arXiv:hep-ph/0512206.
- [16] L. McLerran and R. Venugopalan, *Phys. Rev. D* **49**, 2233, 3352 (1994); **D 50**, 2225 (1994); **D 53**, 458 (1996); **D 59**, 09400 (1999).
- [17] I. Balitsky, [arXiv:hep-ph/9509348]; *Phys. Rev. D* **60**, 014020 (1999) [arXiv:hep-ph/9812311] Y. V. Kovchegov, *Phys. Rev. D* **60**, 034008 (1999), [arXiv:hep-ph/9901281].
- [18] E. Levin and K. Tuchin, *Nucl. Phys.* **A693** (2001) 787 [arXiv:hep-ph/0101275]; **A691** (2001) 779 [arXiv:hep-ph/0012167]; **B573** (2000) 833 [arXiv:hep-ph/9908317]; M. Kozlov and E. Levin, *Nucl. Phys.* **A764** (2001) 498 arXiv:hep-ph/0504146.
- [19] E. Iancu, K. Itakura and L. McLerran, *Nucl. Phys.* **A708** (2002) 327 [arXiv:hep-ph/0203137].
- [20] N. Armesto and M. A. Braun, *Eur. Phys. J.* **C20**, 517 (2001) [arXiv:hep-ph/0104038]; M. Lublinsky, *Eur. Phys. J.* **C21**, 513 (2001) [arXiv:hep-ph/0106112]; E. Levin and M. Lublinsky, *Nucl. Phys.* **A712**, 95 (2002) [arXiv:hep-ph/0207374]; *Nucl. Phys.* **A712**, 95 (2002) [arXiv:hep-ph/0207374]; *Eur. Phys. J.* **C22**, 647 (2002) [arXiv:hep-ph/0108239]; M. Lublinsky, E. Gotsman, E. Levin and U. Maor, *Nucl. Phys.* **A696**, 851 (2001) [arXiv:hep-ph/0102321]; *Eur. Phys. J.* **C27**, 411 (2003) [arXiv:hep-ph/0209074]; K. Golec-Biernat,

- L. Motyka and A. M. Stasto, *Phys. Rev.* **D65**, 074037 (2002) [arXiv:hep-ph/0110325]; E. Iancu, K. Itakura and S. Munier, *Phys. Lett.* **B590** (2004) 199 [arXiv:hep-ph/0310338]. K. Rummukainen and H. Weigert, *Nucl. Phys.* **A739**, 183 (2004) [arXiv:hep-ph/0309306]; K. Golec-Biernat and A. M. Stasto, *Nucl. Phys.* **B668**, 345 (2003) [arXiv:hep-ph/0306279]; E. Gotsman, M. Kozlov, E. Levin, U. Maor and E. Naftali, *Nucl. Phys.* **A742**, 55 (2004) [arXiv:hep-ph/0401021]; K. Kutak and A. M. Stasto, *Eur. Phys. J.* **C41**, 343 (2005) [arXiv:hep-ph/0408117]; G. Chachamis, M. Lublinsky and A. Sabio Vera, *Nucl. Phys.* **A748**, 649 (2005) [arXiv:hep-ph/0408333]; J. L. Albacete, N. Armesto, J. G. Milhano, C. A. Salgado and U. A. Wiedemann, *Phys. Rev.* **D71**, 014003 (2005) [arXiv:hep-ph/0408216]; E. Gotsman, E. Levin, U. Maor and E. Naftali, *Nucl. Phys.* **A750** (2005) 391 [arXiv:hep-ph/0411242].
- [21] Erich Kamke, “*Differentialgleichungen: Lösungsmethoden und Lösung Bd. 1: Gewöhnliche Differentialgleichungen*,” Stuttgart, Germany, Teubner Verlag, 1983.
- [22] Andrey D. Polyanin, “*Handbook of Linear Differential Equations for Engineers and Scientists*”, Chapman & Hall/CRC, 2002.
- [23] H. Risken, “*The Fokker-Planck equation*”, Springer-Verlag, 1989.
- [24] I. Gradstein and I. Ryzhik, “*Tables of Series, Products, and Tables*”, Verlag MIR, Moskau, 1981.
- [25] M. Abramowitz and I. Stegun, “*Handbook of Mathematical Function*”, Dover Publications, Inc., New York, 1972.
- [26] L. N. Lipatov, *Nucl. Phys.* **B452**, 69 (1995).
- [27] A. H. Mueller and B. Patel, *Nucl. Phys.* **B425**, 471 (1994)
- [28] E. Iancu and A. H. Mueller, *Nucl. Phys.* **A730** (2004) 460, 494, [arXiv:hep-ph/0308315], [arXiv:hep-ph/0309276].
- [29] M. Kozlov and E. Levin, *Nucl. Phys.* **A739** (2004) 291 [arXiv:hep-ph/0401118].
- [30] J. Jalilian-Marian, A. Kovner, A. Leonidov and H. Weigert, *Phys. Rev.* **D59**, 014014 (1999), [arXiv:hep-ph/9706377]; *Nucl. Phys.* **B504**, 415 (1997), [arXiv:hep-ph/9701284]; J. Jalilian-Marian, A. Kovner and H. Weigert, *Phys. Rev.* **D59**, 014015 (1999), [arXiv:hep-ph/9709432]; A. Kovner, J. G. Milhano and H. Weigert, *Phys. Rev.* **D62**, 114005 (2000), [arXiv:hep-ph/0004014]; E. Iancu, A. Leonidov and L. D. McLerran, *Phys. Lett.* **B510**, 133 (2001), [arXiv:hep-ph/0102009]; *Nucl. Phys.* **A692**, 583 (2001), [arXiv:hep-ph/0011241]; E. Ferreira, E. Iancu, A. Leonidov and L. McLerran, *Nucl. Phys.* **A703**, 489 (2002), [arXiv:hep-ph/0109115]; H. Weigert, *Nucl. Phys.* **A703**, 823 (2002), [arXiv:hep-ph/0004044].
- [31] E. Iancu and D. N. Triantafyllopoulos, *Nucl. Phys.* **A756**, 419 (2005) [arXiv:hep-ph/0411405]; *Phys. Lett.* **B610**, 253 (2005) [arXiv:hep-ph/0501193].
- [32] A. H. Mueller, A. I. Shoshi and S. M. H. Wong, *Nucl. Phys.* **B715**, 440 (2005) [arXiv:hep-ph/0501088].
- [33] E. Iancu, G. Soyez and D. N. Triantafyllopoulos, arXiv:hep-ph/0510094.
- [34] A. Kovner and M. Lublinsky, arXiv:hep-ph/0510047; arXiv:hep-ph/0503155; *Phys. Rev. Lett.* **94**, 181603 (2005) [arXiv:hep-ph/0502119]; *JHEP* **0503**, 001 (2005) [arXiv:hep-ph/0502071]; *Phys. Rev.* **D71**, 085004 (2005) [arXiv:hep-ph/0501198]; “*Odderon and seven Pomerons: QCD Reggeon field theory from JIMWLK evolution*,” arXiv:hep-ph/0512316.
- [35] Y. Hatta, E. Iancu, L. McLerran and A. Stasto, *Nucl. Phys.* **A762** (2005) 272 [arXiv:hep-ph/0505235]; arXiv:hep-ph/0504182.

- [36] A. H. Mueller and G. P. Salam, *Nucl. Phys.* **B475**, 293 (1996), [arXiv:hep-ph/9605302]; G. P. Salam, *Nucl. Phys.* **B461**, 512 (1996).
- [37] J. Bartels and E. Levin, *Nucl. Phys.* **B387** (1992) 617.
- [38] S. Munier and R. Peschanski, *Phys. Rev.* **D70** (2004) 077503; **D69** (2004) 034008 [arXiv:hep-ph/0310357]; *Phys. Rev. Lett.* **91** (2003) 232001 [arXiv:hep-ph/0309177].
- [39] A. H. Mueller and D. N. Triantafyllopoulos, *Nucl. Phys.* **B640** (2002) 331 [arXiv:hep-ph/0205167]; D. N. Triantafyllopoulos, *Nucl. Phys.* **B648** (2003) 293 [arXiv:hep-ph/0209121].
- [40] K. G. Boreskov, “*Probabilistic model of Reggeon field theory*,” arXiv:hep-ph/0112325 and reference therein.
- [41] D. Amati, M. Le Bellac, G. Marchesini and M. Ciafaloni, *Nucl. Phys.* **B112** (1976) 107; D. Amati, G. Marchesini, M. Ciafaloni and G. Parisi, *Nucl. Phys.* **B114** (1976) 483.
- [42] Le-Wei Li, Xiao-Kang Kang and Mook-Seng Leong, “*Spheroidal Wave Functions in Electromagnetic Theory*”, Jon Wiley & Son Inc. 2002.
P. Falloon, “*Homepage of the Spheroidal Wave Functions*.”
<http://www.physics.uwa.edu.au/falloon/spheroidal/spheroidal.html>;
- [43] M. Kozlov, E. Levin and A. Prygarin *in preparation*.
- [44] V. Khachatryan and E. Levin, *in preparation*.
- [45] Y. V. Kovchegov, *Phys. Rev. D* **72** (2005) 094009 [arXiv:hep-ph/0508276].
- [46] A. H. Mueller and A. I. Shoshi, *Nucl. Phys.* **B692** (2004) 175 [arXiv:hep-ph/0402193].
- [47] E. Ferreiro, E. Iancu, K. Itakura and L. McLerran, *Nucl. Phys. A* **710** (2002) 373 [arXiv:hep-ph/0206241]; E. M. Levin and M. G. Ryskin, *Phys. Rept.* **189** (1990) 267.
- [48] O. V. Kancheli, “*About the structure of the Froissart limit in QCD*,” arXiv:hep-ph/0008299.